8-10-2005

3D Seismic Interpretation of Turbidite-Sands from the Gulf of Mexico

Omar Akbar
University of New Orleans

3D SEISMIC INTERPRETATION OF TURBIDITE-SANDS FROM THE GULF OF MEXICO

A Thesis

Submitted to the Graduate Faculty of the
University of New Orleans
in partial fulfillment of the
requirements for the degree of

Master of Science
in
The Department of Geology and Geophysics

by

Omar Othman Akbar

BS. King Fahid University of Petroleum and Minerals, 1994

August 2005


الحمد لله والشكر لله
ولا إله إلا الله
والله أكبر

ACKNOWLEDGMENT

This is the most difficult part to write in my thesis. Thanking people who contributed to my success is not an easy task. Many people helped and supported me to reach this stage. I will try my best to pass my deepest thanks in a few words, but I know what they gave me is much more than words to be written. First, I would like to thank Saudi Aramco for giving me this opportunity to get my advanced degree in Geology. I would also like to thank my manager Saad Al-Akeel for his encouragement and support. Thanks to my colleagues at Aramco who took over my workload and made this scholarship possible. Lastly, I would like to thank my Aramco advisors Brad Brumfield for his understanding and support for the last two years.

At UNO, I was also surrounded by great people. Thanks to Dr. Mostofa Sarwar for sharing his knowledge and guiding me during my research. Thanks for being so patient and kind with me. I would also like to express my deepest gratitude to Dr. Laura Serpa, who has been my mentor and guide since the very beginning of my program. She was a great adviser in helping me to select the right courses at the right times. My accomplishments could not be possible without her support and advice. Thanks to Dr. Mathew Totten for being part of my committee

and for his opportune advice. Thanks to all my teachers and my friends at UNO, who contributed to this accomplishment.

Finally, I would like to pass my greatest appreciation to Ibrahim AlQassim, who gave me my first hand in the United States and continued to offer his help whenever I need it.

Everyone wants to be in the picture, but me.
For the past two years I was out of this picture. I was busy with my study and research.
Now it is the time to tell my family

THANK YOU …….. FOR BEING SO PATIENT

I am back,
Omar Akbar

TABLE OF CONTENTS

ABSTRACT

This thesis interprets and maps some key stratigraphic and structural elements of Garden Bank (GB) Block 191 applying both geological and geophysical techniques. The area is located in the Gulf of Mexico 160 miles southwest of Lafayette. Three-dimensional seismic data and some well logs were integrated and analyzed to construct a reasonable geological subsurface image. GeoFrame software from Schlumberger was used in this research. A spatial attention was given to salt diapers. Their influence on sand accumulations and hydrocarbon traps were investigated. Two Pleistocene sands accumulations (4500-ft & 8500-ft) were examine thoroughly in this research. Time and amplitude maps were produced. In addition, a wave-theoretical model that describes salt tectonic activities within the area was reconstructed in order to understand the influence of these dynamical forces on the overlaying strata.

CHAPTER 1: INTRODUCTION

1.1 Area Overview

The Gulf of Mexico basin is a semi-circular structure of 1,500Km in diameter. It is filled with sedimentary rocks that range in age between Triassic to Holocene. The uppermost Middle Jurassic is famous with its extensive salt deposition that is prevalent over most of the Gulf of Mexico. Overlaying the salt is a very thick sequence of sediments deposited mostly in marine environments (Salvador, 1991).

Salt is one of the most effective agents in nature for trapping oil and gas. Salt flows when overlaying sediment's density exceeds that of salt. Another driver for salt to flow is related to differential sediment loading over salt or to gravitational forces due to surface slope (Nelson, 1991). As a ductile material, salt can move and deform surrounding sediments, creating traps. Salt is also impermeable to hydrocarbons and acts as a seal. Most of the hydrocarbons in North America are trapped in salt-related structures (Farmer, et al., 1996).

Salt movement immensely influenced the structure and lithology of Garden Bank (GB) Block 191. The area is located in the Gulf of Mexico 160 miles southwest of Lafayette (Figure 1.1). It is between Texas-Louisiana outer shelf and Texas-Louisiana upper slope and is at a water depth of 700 ft. Two Pleistocene

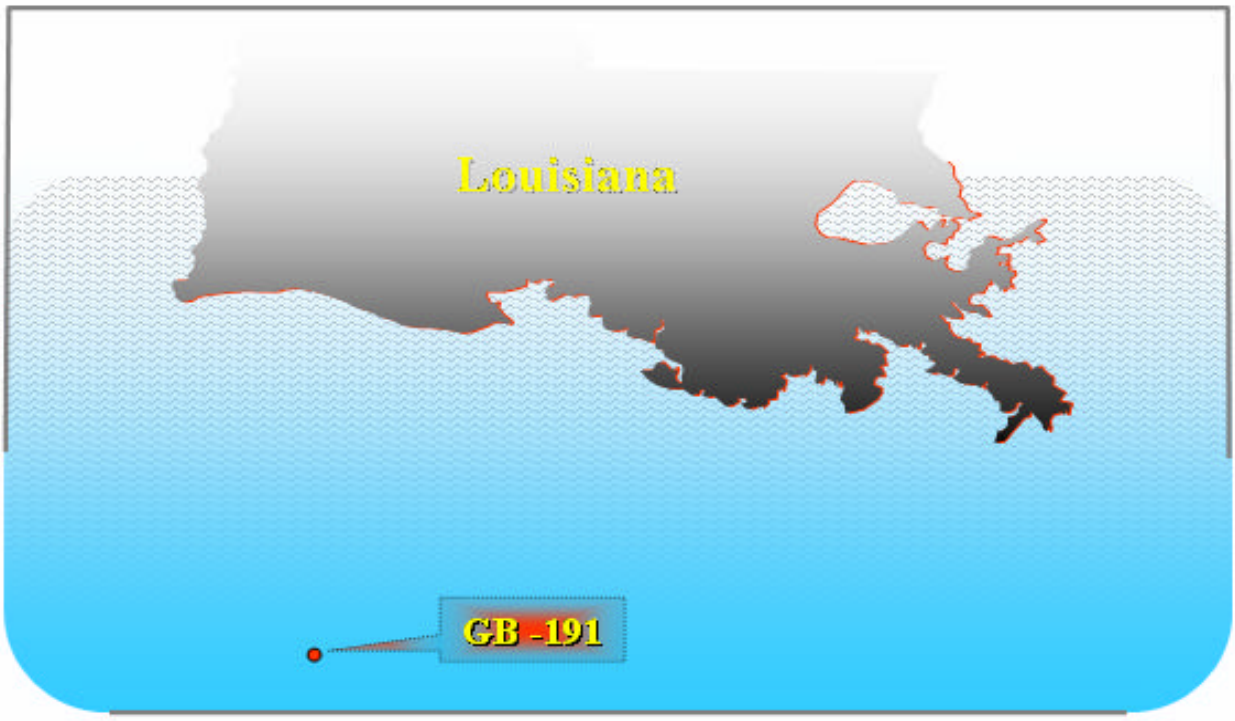

Figure 1.1: Garden Bank 191, site location

sands (4500-ft and 8500-ft) were deposited during relatively regressive sea level. The Sands were transported to the area from some deltas to the north of GB-191 (Figure 1.2). These shelf edge deltas are 10-15 miles to the north of GB-191, where they constitute the main reservoirs at West Cameron 638 and 643 fields (Fugitt et. al., 2000).

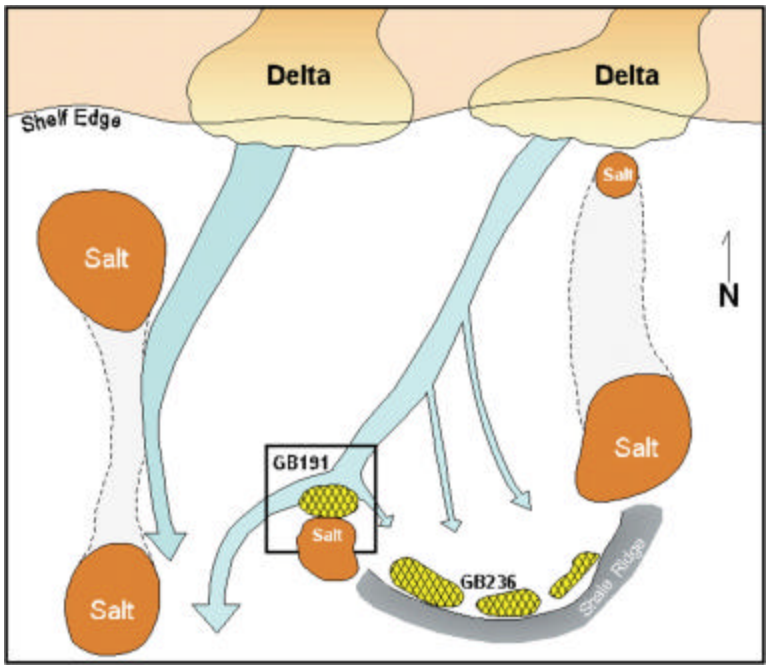

Figure 1.2: Depositional model by Fugitt et. al., 2000.

The information about these oil reach areas is meager. Surface and subsurface mapping are important for geologists to understand the earth and reconstruct history. But detailed subsurface mapping has extra benefits as it relates more to oil and gas exploration. Oil and gas industries spend a considerable amount of resources to generate subsurface maps. Usually these maps stay confidential. This thesis provides detailed structural maps and gives an integrated wave-theoretical model of my study area which would help understand the geologic events that led to hydrocarbon accumulation in the area.

1.2 Thesis Objective

The objective of this thesis is to study the 4500-ft and 8500-ft sands accumulations in GB-191, and to examine how they were impacted by salt tectonics. I believe that this study would lead to a better understanding of hydrocarbon traps by integrating both geological and geophysical data within the area. Some results this thesis will be presented as time and amplitude maps (time maps provide structural information while amplitude maps provide stratigraphic and reservoir information). Also, this thesis will reconstruct a wave-theoretical model that describes sand accumulation and its relationship to salt evolution.

1.3 Thesis Significance

The significant benefits of this study are to enrich our understanding of GB191 geological history and to provide detailed and comprehensive analysis of the Pleistocene sands deposition. The result of this project can provide clues to potential prospects and leads in the area. Finally, the interpreted data can be used for seismic attribute analysis, quality enhancement and time to depth conversion.

An important aspect of this study is to produce an integrated data set extracted from different sources and put them in format ready to be used

under the GeoFrame environment. Students and staffs can utilize these data and enhance them without the need to go through a lengthy process of data collection and management.

A knowledge database was built and posted on the supervisor's webpage. The database put together information about area history, geological interpretation, previous studies, well information, and production history. Such information is essential for any similar study in the future.

1.4 Previous Work

There is only one published interpretations about GB-191. The interpretations were published in The Leading Edge (April 2000) by Fugitt et. al. The paper stated that both salt and Plio-Pleistocene-age shale mobilized into diapirs and ridges due to rapid sediment loading. The diapirs formed topographic highs and lows on the slope trapping sand that were transported downslope from deltas located in the north. These sands were trapped on the north flank of a salt diapir in Block 191. The 4500-ft and 8500-ft intervals were rotated and gas was trapped by the updip shale-out (stratigraphic trap formed by increases in clay content until porosity and permeability disappear) of the sands to the south (Figure 1.3) as the mini-basin on the north flank continued to subside due to continued loading and withdrawal.

The paper published two maps on the 4500-ft and 8500-ft sands (Figure 1.4 and 1.5). One map shows that the 4500-ft sand accumulation is trapped on a north plunging nose by stratigraphic shale-outs and faulting to the south, west, and east. The other map shows the 8500-ft sand as a localized channel in a small withdrawal basin to the north of the salt dome.

This thesis study differs than Chevron work (Fugitt et. al., 2000) by paying more attention to salt evolution in the area. The influence of salt dynamics on overlaying beds and their direct relationship with the fault system are the core element of this thesis. The maps produced are in time and cover the whole extent of the GB-191. In addition, a detailed depositional model was developed that would help reconstructing the history of the area.

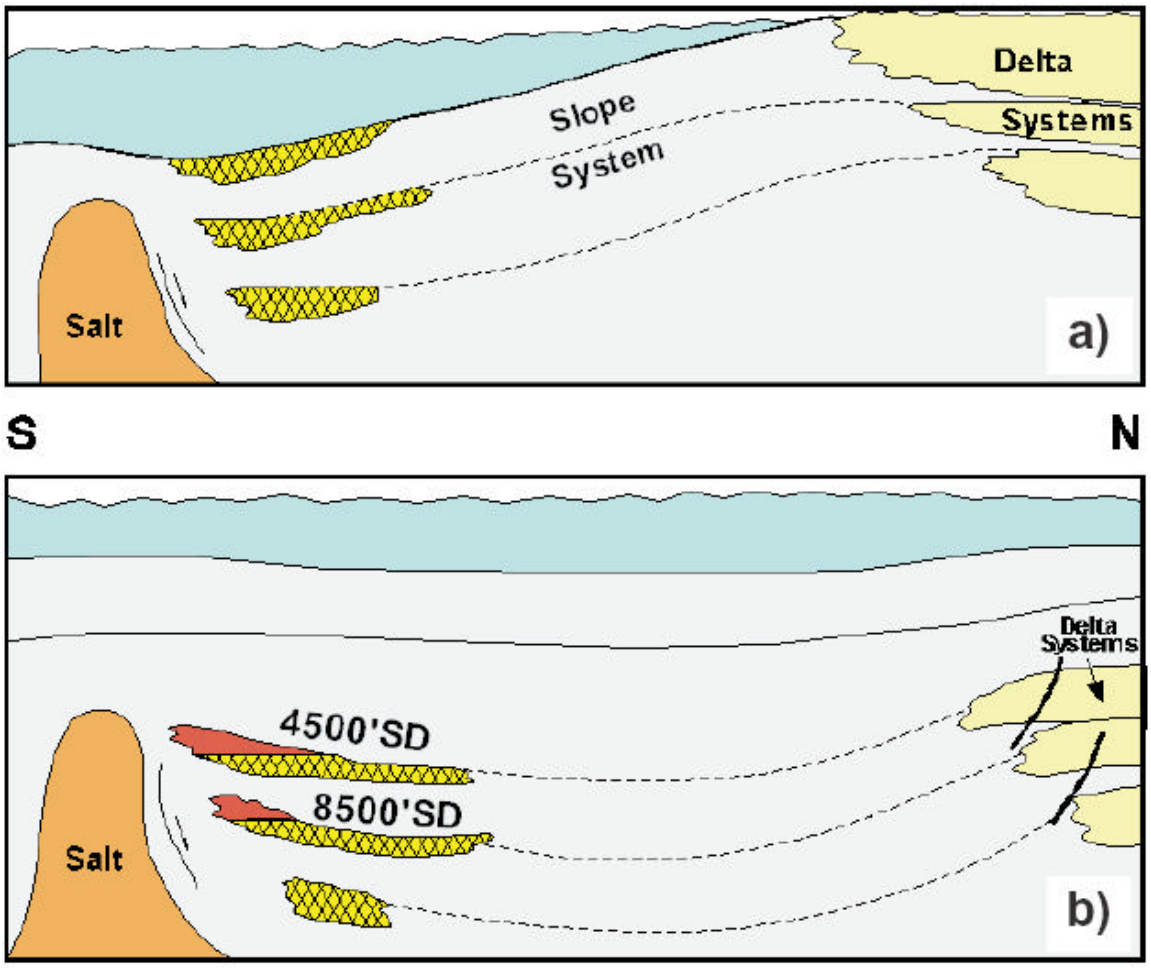

Figure 1.3: Depositional model Garden Banks 191 (cross-sectional view). Sand was trapped on the north flank of a salt diapir at block 191. As the north flank minibasin continued to subside (a) due to continued loading and withdrawal, the 4500-ft interval was rotated, and gas was trapped (b) by the updip shaleout of the sand to the south (Fugitt et. al., 2000).

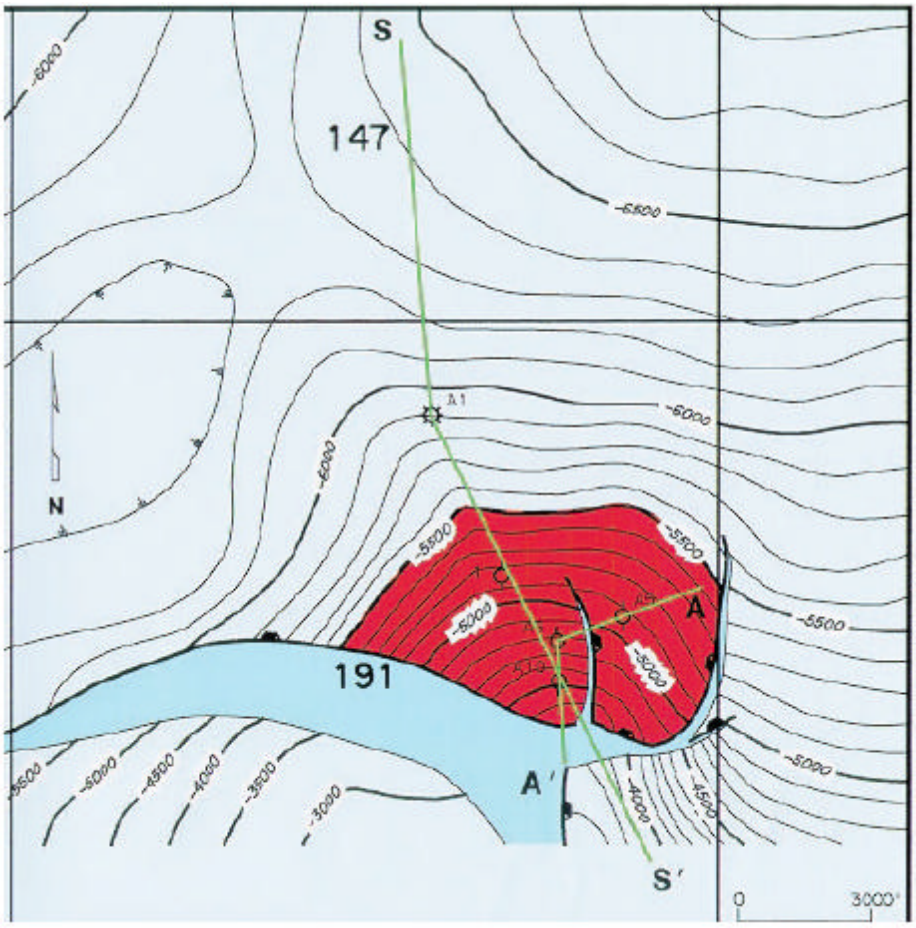

Figure 1.4: Depth map of the 4500-ft sand. (Fugitt et. al., 2000).

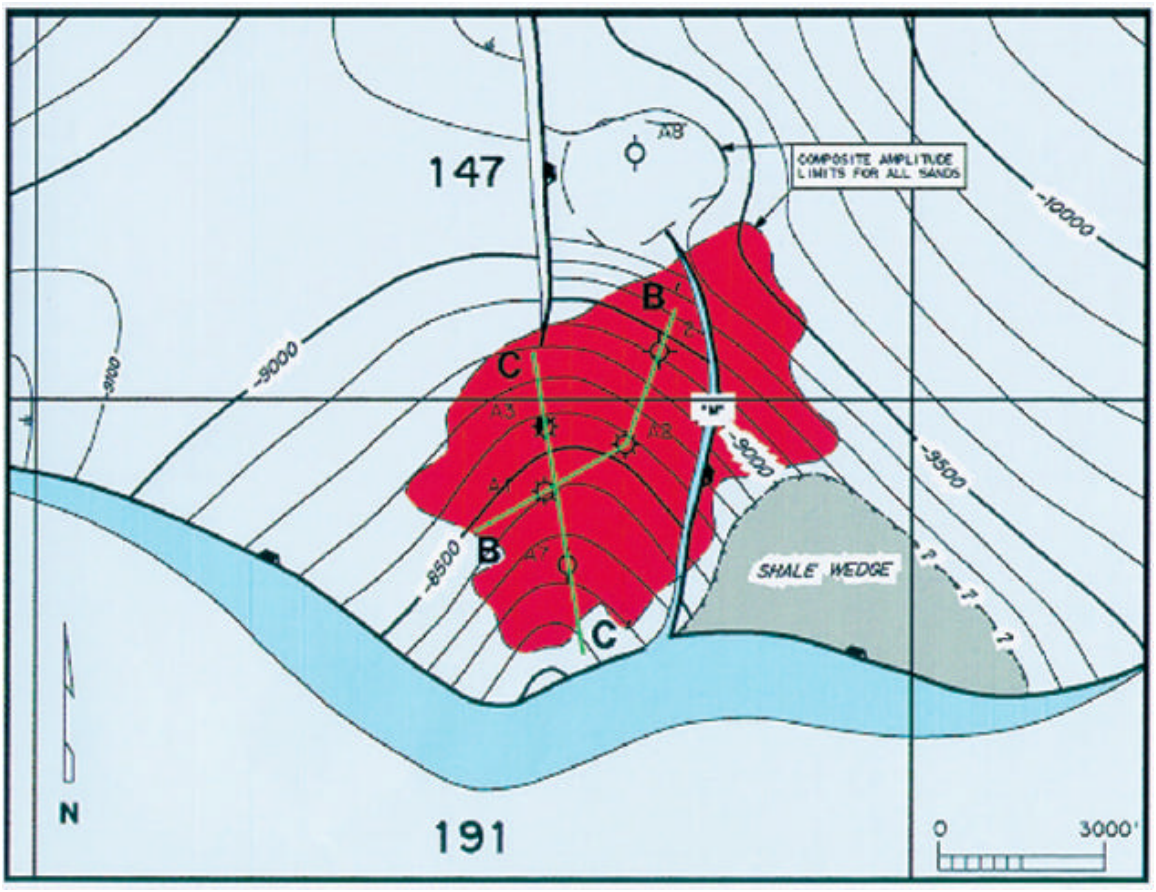

Figure 5: Depth map of the 8500-ft sand. (Fugitt et. al., 2000).

CHAPTER 2: METHODOLOGY

Interpretation is like art. Although it has some general guidelines, each interpreter has his own world of creativity. Interpreters utilize different types of computer tools to generate scientific maps that help in hydrocarbon exploration and production. These tools allow them to draw lines, squares and polygons. Also, they provide a way to slice seismic in different directions and visualize data in two and three dimensional view. Interpreters expect from interpretation tools all basic functions that they can find in *Microsoft Paint* and some 3D capabilities similar to what available in *AutoCad.*

As a new interpreter, adhering to the basic interpretation guidelines and applying them in this thesis by using workstation-baseed tools is essential in establishing my interpretation skills. This chapter will go over these guidelines and relate them to GeoFrame/IESX; a seismic interpretation tool from Schlumberger. The information to be presented here is crucial for those who are seeking to do future work in seismic interpretation. Extra information about IESX can be found in GeoFrame Book-Shelf, which comes with the software installation. Also, a quick and easy reference is available at:

http://www.ldeo.columbia.edu/BRG/ODP/ODP/IESX.

2.1 Study and evaluation of the Area

Any interpretation, within a new area, starts with general study and evaluation. This step was important to boost my knowledge in the geology of the area. I was interested in collecting information about previous studies, area's dominant structures, depositional models, well reports, production history and old geological maps. Lots of data analysis and evaluation applied at this stage. Due to the complexity of the area's subsurface-structures, I had to do some extra studies to understand salt and shale tectonics, which are the main structures within the Gulf of Mexico basin. There are significant literatures that cover this subject. Thomas Nelson wrote several reviews about salt tectonics in the Gulf of Mexico that helped me tremendously during my works.

2.2 Data Collection

To carry out a seismic interpretations process, access to seismic data is essential. Availability of other data may enhance the quality of the interpretation. Unfortunately, not all desired data can be accessed. Due to the competitions between oil companies, some data are kept confidential.

The seismic data I used in this study was a donation from Diamond Geosciences Research Corporation. For other data, I had to depend on public sources. Minerals Management Service (MMS) publishes a fair amount of field and well data. Theses data are at least two years old and some time with poor

quality. The good thing about these data, however, is their ease of access. These data are available online and can be downloaded from http://www.gomr.mms.gov.

After downloading, data were filtered, manipulated and integrated. MMS provides data in huge files, sometime exceeding 0.5 GB. Such files can't be viewed with regular text editor. In addition, required information can be scattered between different files, and these files can be of different format, such as PDF, TXT and XLS. Therefore, I had to build some scripts (computer programs) to extract information from these files and to integrate them in a useful format.

I used "Perl" to build these scripts. Perl is a powerful scripting language widely used for file editing and manipulation. It is installed on all UNIX systems that are available at UNO. Perl needs to be installed for Windows systems. It is offered for free at: http://www.ActiveState.com/ActivePerl. Extensive online documentation is included with Perl installation. Also, there are several good books about Perl. The premier book on ActivePerl for Windows is "Learning Perl on Win32 Systems" by Schwartz, Olson, and Christiansen (O'Reilly & Associates, 1997). For Perl in general, two books to consider are "Programming Perl", 3rd Edition, by Larry Wall, Tom Christiansen and Randal L. Schwartz (O'Reilly & Associates, 1996) and "Learning Perl", 3rd Edition, by Randal L. Schwartz (O'Reilly & Associates, 1993).

I published all data used in my thesis at: http://www.geology.uno.edu/GInt/index.html. These data were filtered and manipulated to satisfy the requirements of the study. In addition, the webpage includes the Perl scripts used in generating these data. Following is a list of all data utilized in the thesis:

- 3D Seismic data in time domain
- Sonic, density, resistivity, spontaneous potential (SP) and gamma ray (GR) well logs
- Well coordinates
- Well headers (total depth, water depth, run date, kelly bushing and well status).
- Paleo-reports and perforated intervals.
- Directional survey points.
- Velocity surveys.
- Wells productions.

2.3 Geological Interpretations

Well Logs help define physical rock characteristics such as lithology, porosity, pore geometry, and permeability. Logging data is used to identify productive zones, to determine depth and thickness of zones, to distinguish between oil, gas, or water in a reservoir, and to estimate hydrocarbon reserves.

In geological interpretation process, well logs are used to correlate zones of similarity between different wells. This assists to build structural and stratigraphic maps and cross sections. Although, this process in not essential to my thesis, it helped in enhancing my knowledge about the area and put additional constrains on my seismic interpretations.

Paper-based log correlation techniques have been the basic tools utilized by geologist for over 50 years (Tearpock and Bischke, 2003). Currently, computer-based log correlation is more common. In this thesis, I used the paper-based correlation technique due to two reasons: (1) not having accesses to well logs in a format that is loadable to interpretation software, and (2) lack of experience in digital correlation tools.

2.3.1 Data preparation

MMS provides well logs data in "tiff" format. Every log is about 1 ft wide and more than 8 ft long. Not all software can open these log files efficiently. "Imaging" from Microsoft is the best software, available at UNO, to view these logs. Before correlation, logs need to be plotted on large papers. The Geology Department doesn't have plotters that are specialized in log printing. Available printers are 3 ft long. That means lot of papers will be wasted by printing the tiff files without editing. Therefore, Adobe Illustrator was used to rearrange the data in

three columns in order to plot them. Finally, plotted logs are cut and folded. Figure 2.1 summarizes this process.

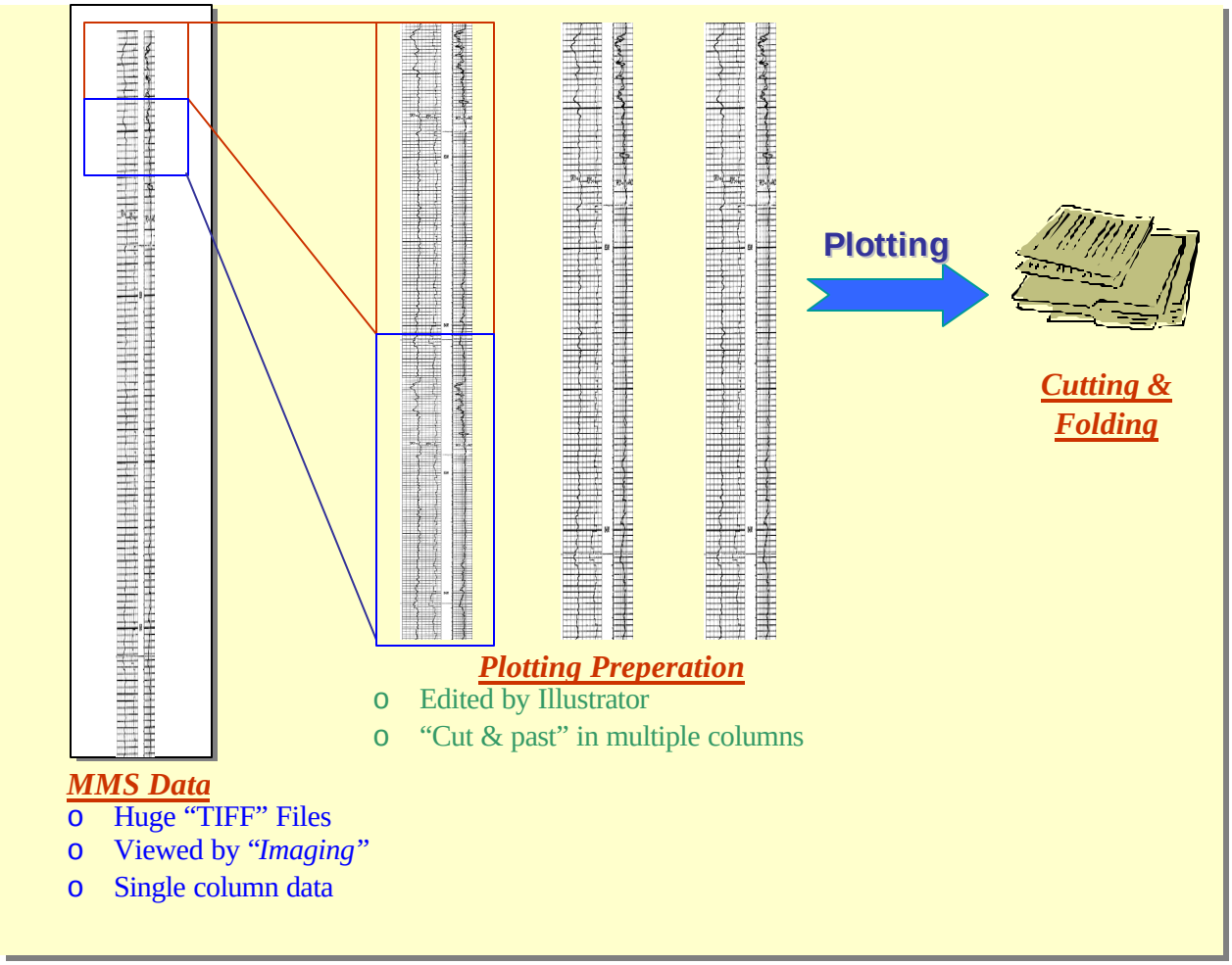

Figure 2.1: Data Preparation

2.3.2 Log Correlation

Log Correlation is similar to pattern recognition. When geologists correlate one log to another, they are attempting to match the pattern of curves on

one log to the pattern of curves found on the second log. For correlation work, it is best to correlate well logs that have the same type of curve and processed by the same operator. However, this is not always possible, spatially with public data.

Figure 2.2 illustrates two logs for a single well (A002) from GB-191. Both logs display GR and Resistivity curves, but from two different operators. The differences in magnitude of fluctuations are clear between the two logs. Therefore, the correlation work must be independent of the magnitude of the fluctuations and the variety of curves on the individual well logs.

Data presented on well log are representative of the subsurface formations found in the well-bore. A correlated log provides information about the subsurface, such as stratigraphic markers, tops and base of stratigraphic units, depth and amount of missing or repeated section resulting from faults, lithology, depth to and thickness of hydrocarbon-bearing zones, porosity and permeability of productive zones, and depth to unconformities (Tearpock and Bischke, 2003). Example of logs representation is illustrated in Figure 2.3.

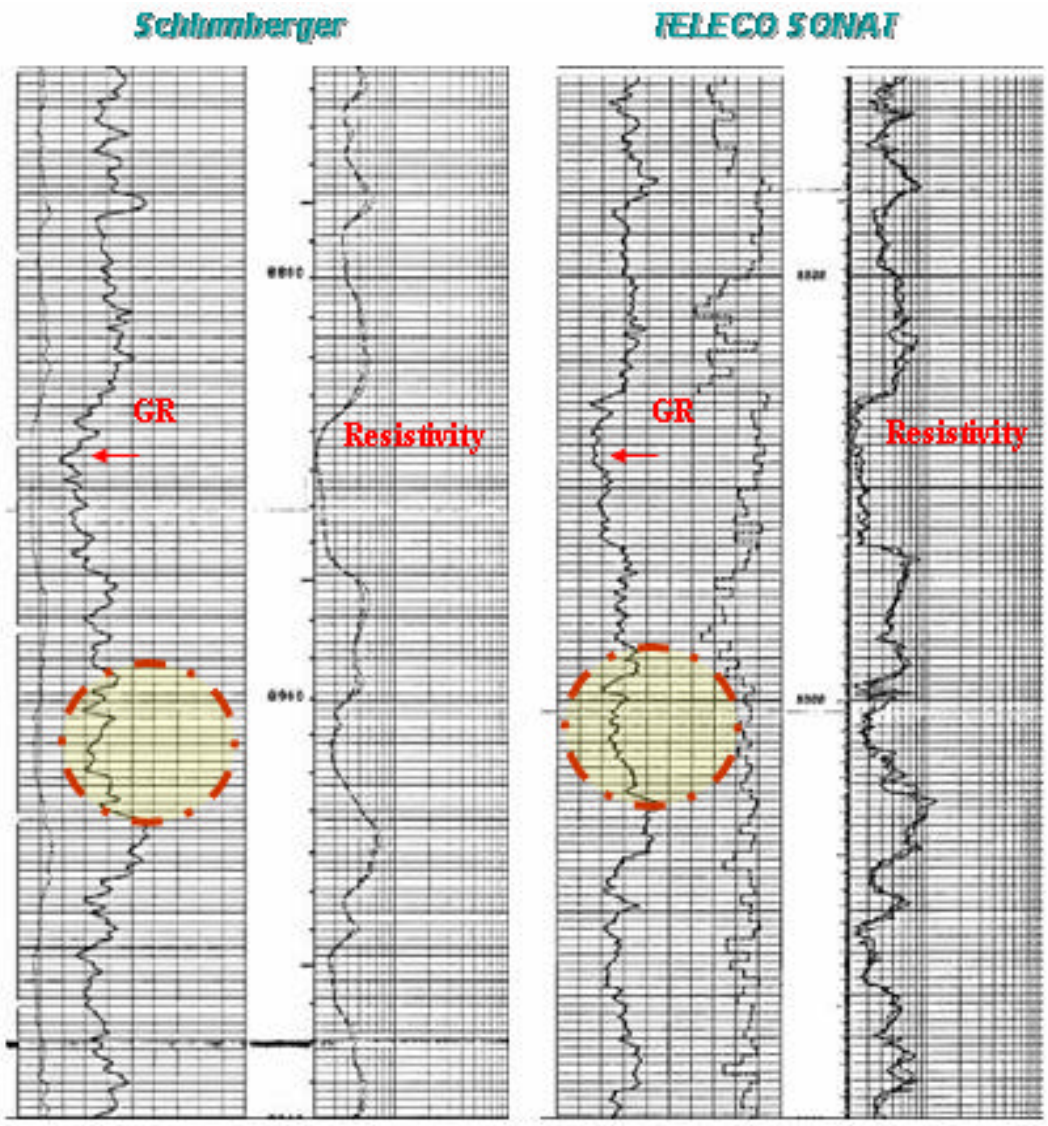

Figure 2.2: ***Well***: A002 ***API***: 608074062402 *Area*: GB-191

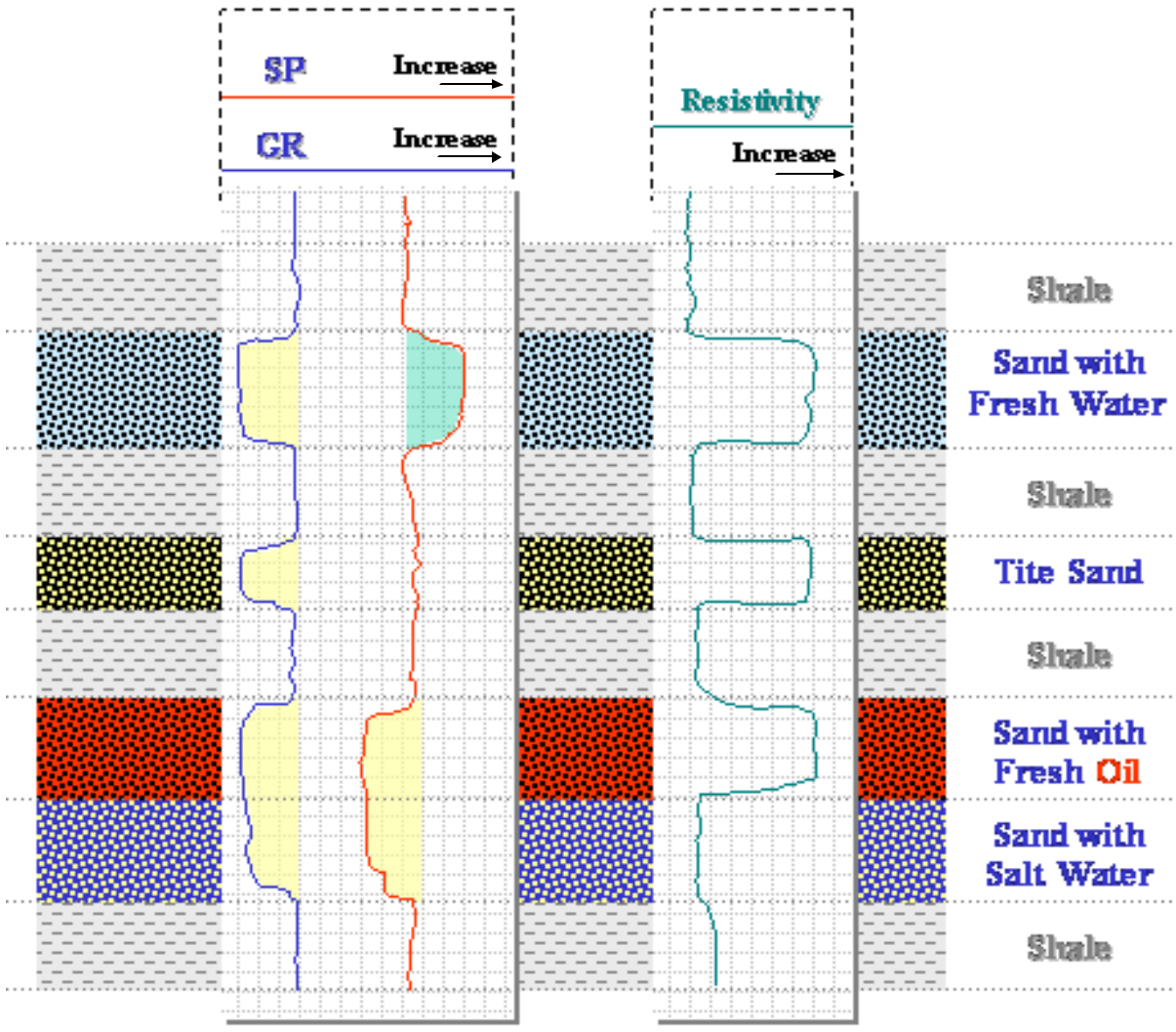

Figure 2.3: General Well logs representation.

In this thesis, seven wells from GB-191, that targeted the two production sands, are evaluated. A002 ST1, A004 and A007 are wells that produced gas from the 8500-ft sand, while A005, A006, A009 and A010 produced gas from the 4500-ft sand. I correlated the 4500-ft producing wells separately from the other ones. Example of the correlation is shown in Figure 2.4. Table 2.1 and 2.2 summarize the geological interpretation results.

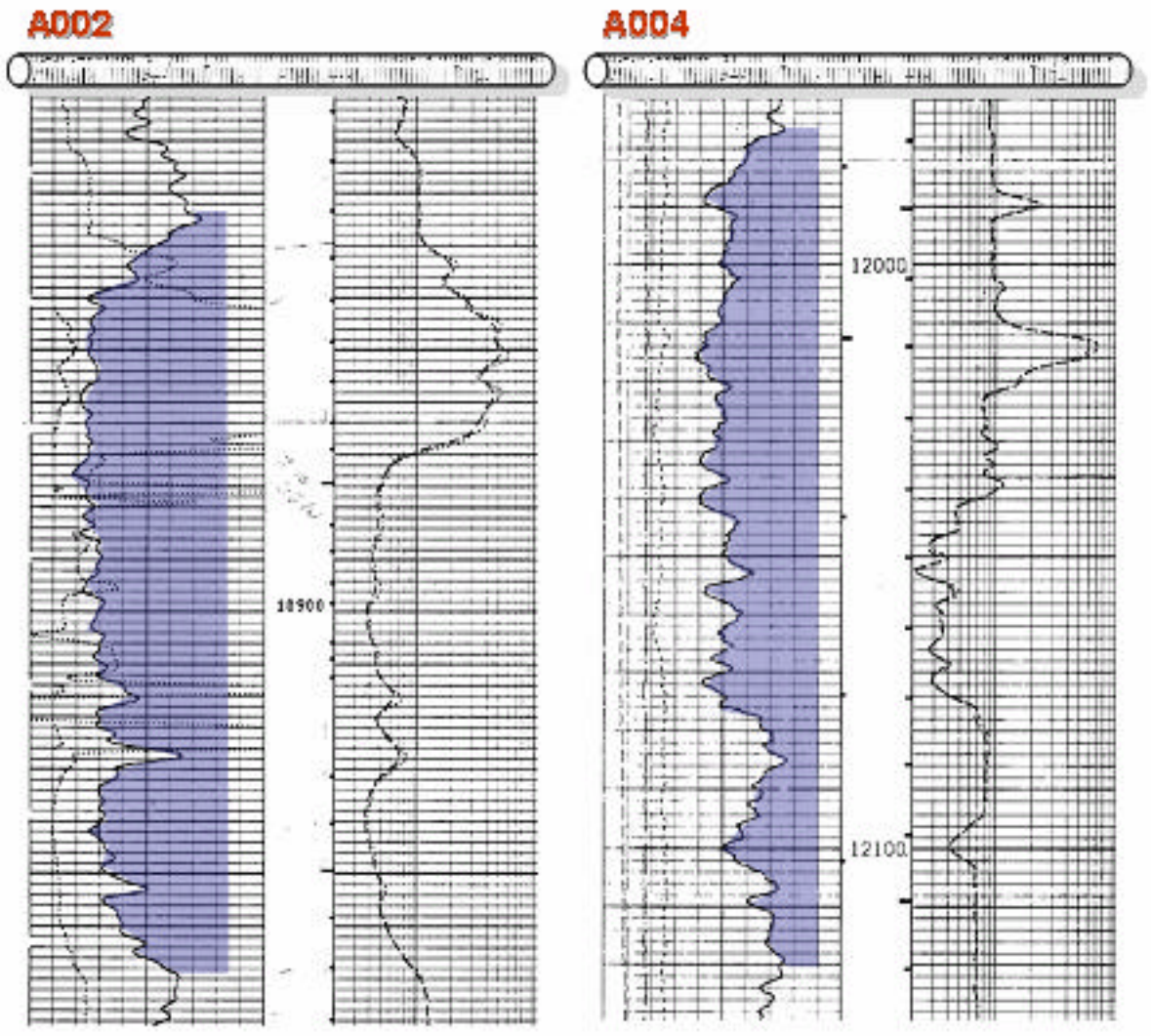

Figure 2.4: Log correlation, showing middle of member 3 for the 8500-ft sand.

Table 2.1: Well correlations for the 8500-ft sand.

Well Name	A2ST1	A4	A7
API Number	608074062402	608074013300	608074012800
8500 - 2 **TOP**	MD: 10550	MD: 11604	--
BASE	MD: 10646	MD: 11700	--
8500 - 3 MID **TOP**	MD: 10814 TVD: 8678	MD: 11978 TVD: 9252	MD: 9538 TVD:8181
BASE	MD: 10954	MD: 12084	MD: 9634
8500 - 3 LWR **TOP**	MD: 10960	MD: 12086	MD: 9638
BASE	MD: 11082	--	MD: 9974
8500 - 4 **TOP**	MD: 11092	--	MD: 9980
BASE	MD: 11354	--	MD: 10250

Table 2.1: Well correlations for the 4500-ft sand

Well Name	A005	A006	A009	A010
API Number	608074012800	608074013200	608074012900	608074064700
4500 - 1 **TOP**	MD: 5738 TVD: 5152	MD: 5108 TVD: 4847	MD: 7932 TVD: 4471	MD: 5280 TVD: 4694
BASE	5918	5314	8252	5410
4500 - 2 **TOP**	MD: 5918 TVD: 5271	MD: 5314 TVD: 5053	MD: 8252 TVD: 4605	MD: 5410 TVD: 4820
BASE	MD: 6112 TVD: 5440	MD: 5418 TVD:5257	MD: 8592 TVD: 4766	MD: 5556 TVD: 4961
4500 - 3 **TOP**	6112	5418	--	5556
BASE	6378	5612	--	5636
4500 - 4 **TOP**	6416	5628	--	5658
BASE	6490	5734	--	5700
Fault 1	MD: 270/5918/A9 TVD: 129/5271/A9	MD: 270/5314/A9 TVD: 129/5053/A9		MD: 270/5410/A9 TVD: 129/4820/A9

2.3.3 Map Generation

The information obtained from correlated logs is the raw data used to prepare subsurface maps. The maps may include fault, structure, stratigraphic, salt, unconformity, and variety of isochron maps. Usually, these maps are constructed for specific stratigraphic horizons to show, in plan view, the geometric shapes of these horizons. Correlated information can also be used to prepare a variety of cross sections.

The number of wells drilled in GB-191 is too low to generate detailed subsurface maps. But as I mentioned earlier, the objective of the geological interpretation step, in this study, is to enhance my knowledge of the area and to have more well controls over the seismic data, by marking all perforated intervals and sand limits. Therefore, I built some basic stratigraphic maps to guide me in my seismic interpretation task (Figure 2.5 and 2.6).

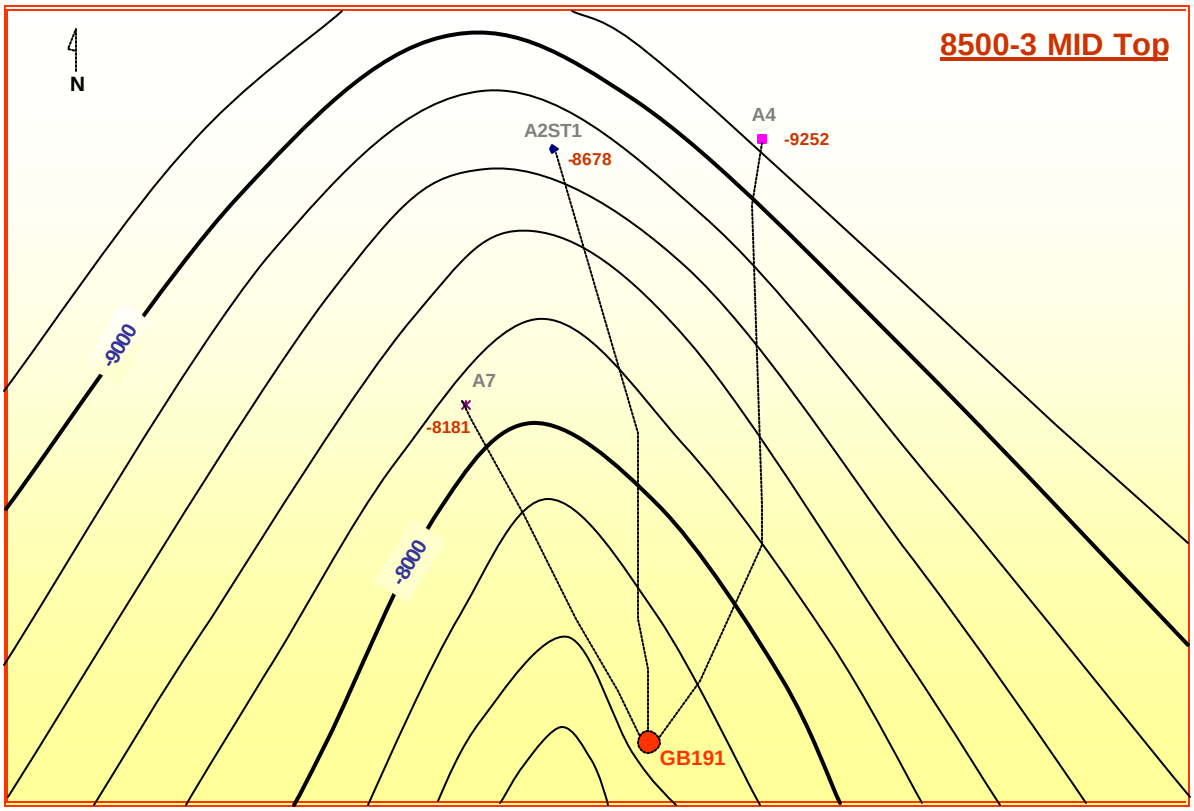

Figure 2.5: Top of member 3 for the 8500-ft sand map.

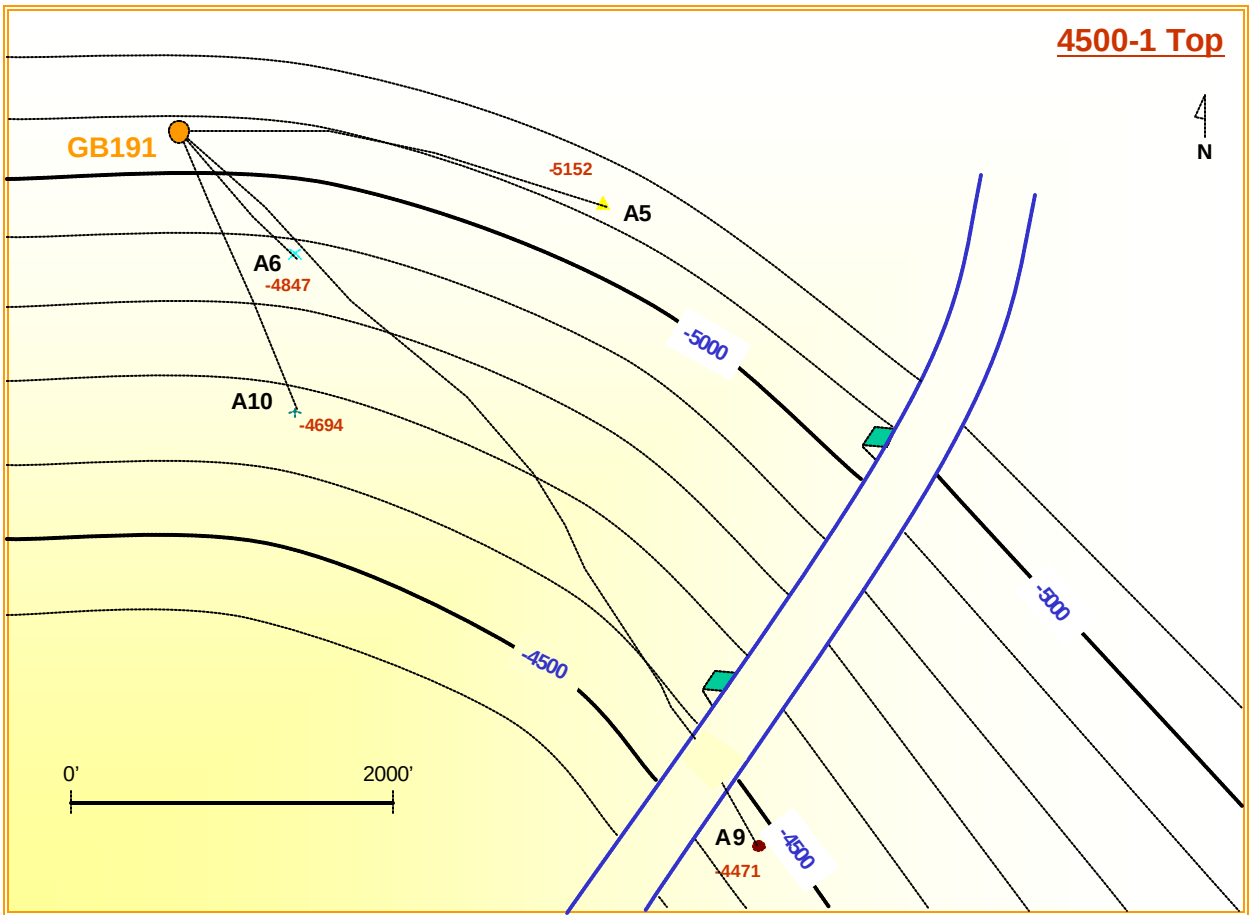

Figure 2.6: Top of member 1 for the 4500-ft sand map.

2.4 Geophysical Interpretation

After seismic acquisition, data are processed to produce a subsurface image. The image is then interpreted on computers using seismic interpretation software. The result is a map of the subsurface geology. From this interpretation and map come the decision on where to drill. The seismic interpretation software used in this thesis is GeoFrame/IESX from Schlumberger. IESX allows interpreters to quickly combine 2D and 3D seismic surveys and well data into a single project.

2.4.1 Data Loading

GeoFrame is the Schlumberger umbrella that integrates all geological and geophysical applications and data. IESX is one of these applications that GeoFrame controls. GeoFrame utilizes Oracle to store data while part of IESX still uses binary files. The reason behind that is that IESX deals with seismic data, which are huge in size and can't be stored efficiently in Oracle. Well data, however, are stored in Oracle. Synchronization between Oracle and the binary files is essential to keep the data safe.

Processed data are commonly available in SEGY format. In order to access seismic data by interpretation software, SEGYs are needed to be loaded. Although, IESX provides some tools to help in loading seismic, this is a time consuming process and is prone to error. Of special concern is the fact that position errors may go undetected and may result in an erroneous interpretation.

Seismic and well data can be loaded into IESX from "*IESX Data Manager*" (Figure 2.7). This can be launched from *IESX Session Manager* → *Application*→*Data Manager*. Loading well data is straightforward. *IESX Book Shelf* explains the loading steps in a simple way. I published all files I used to load well data at: http://www.geology.uno.edu/GInt/index.html. These files are in IESX loadable format. Loading seismic data, however, is quite complicated. To simplify this process for future students, I loaded six blocks of Garden Bank seismic data into IESX (191, 192, 193, 235, 236 and 237). The data loaded in a project named "***GB_master***". Students who want to access this data need to share them from *IESX Data Manager/ Share* (Figure 2.8). The list in the upper left corner shows all GeoFrame projects. When you select "***GB_master***", you are prompted for the password to this project. The survey volume present in this project will appear. Select that volume and then press "*Share*". This operation will take few seconds and you will then have a read access to the seismic.

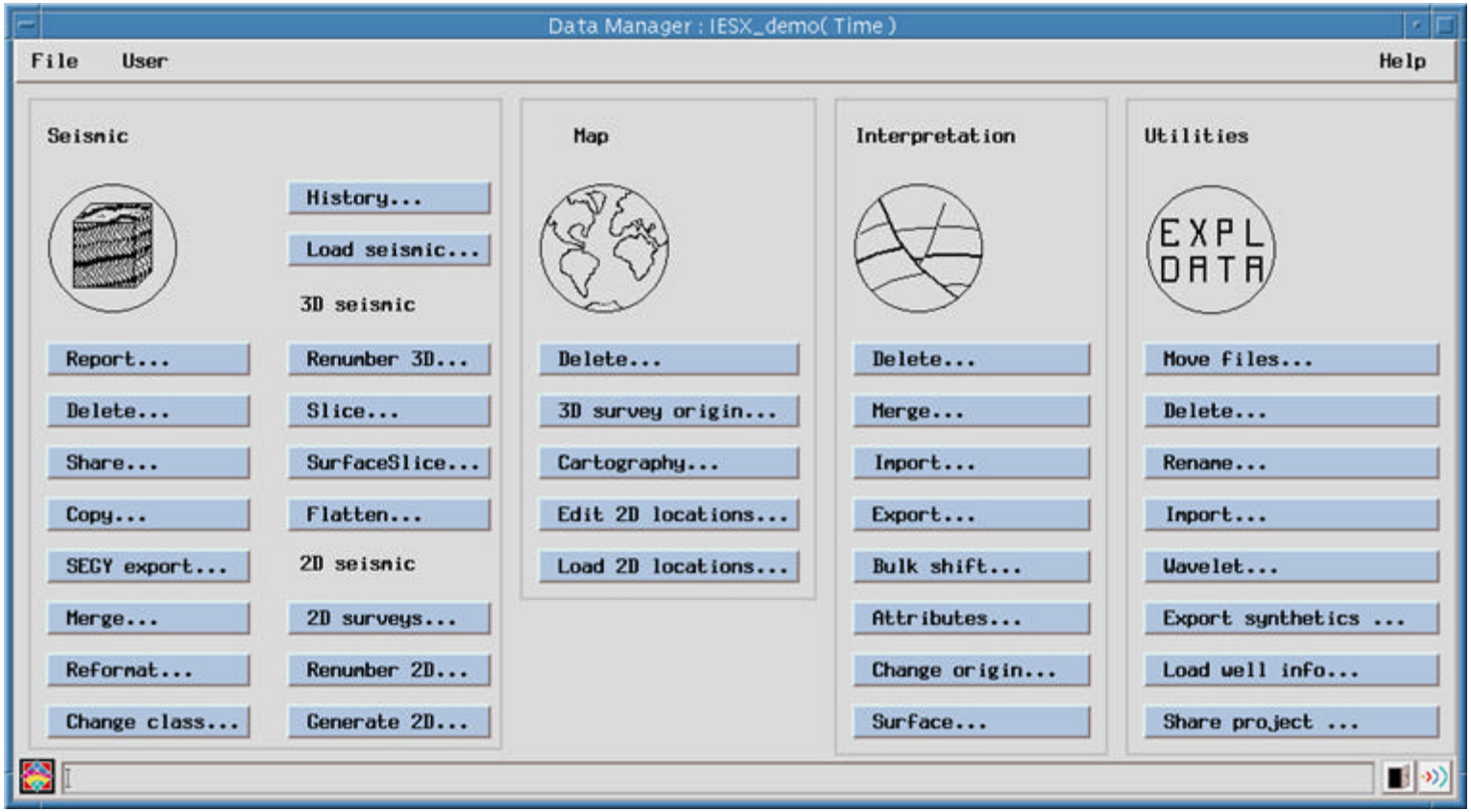

Figure 2.7: IESX Data Management

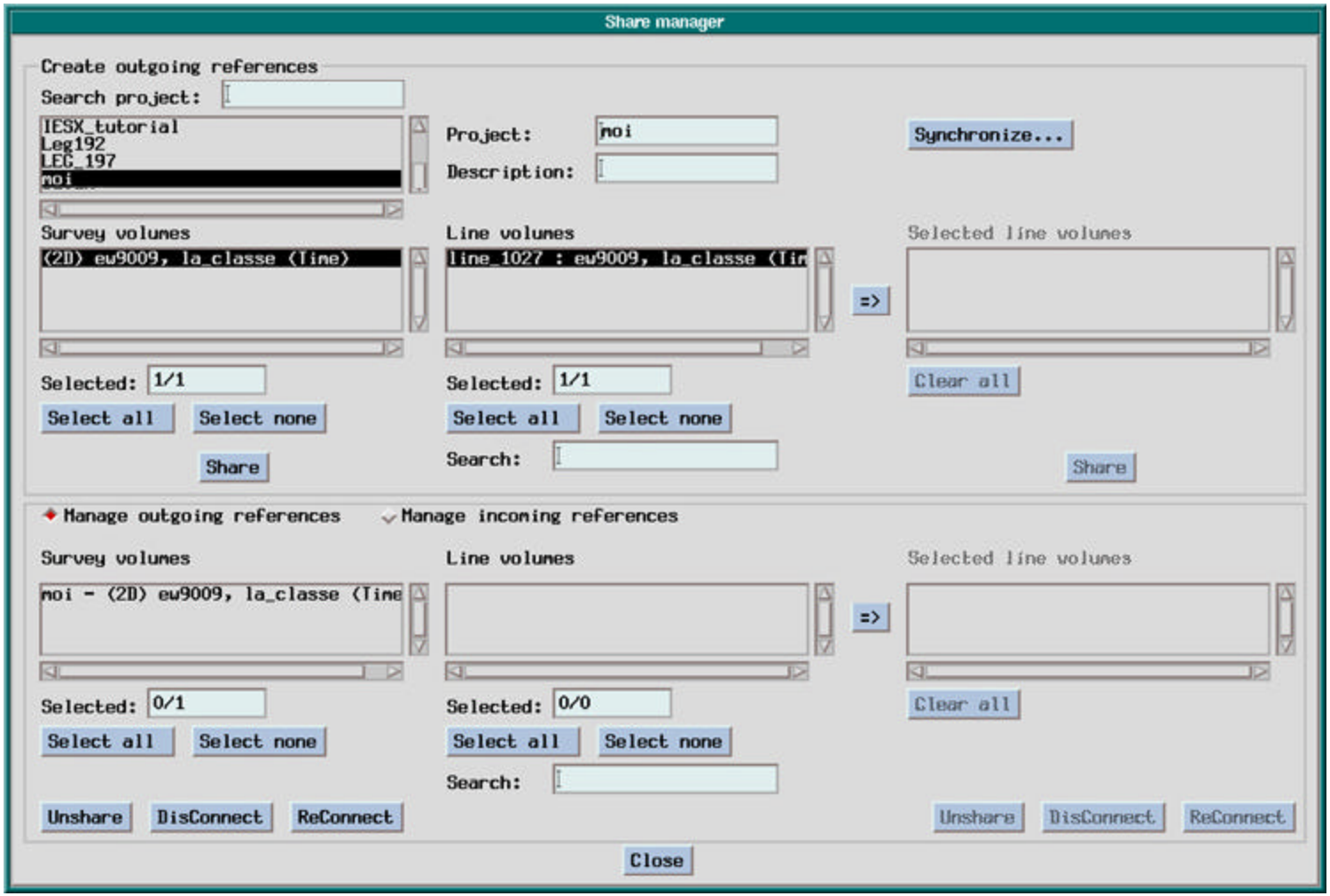

Figure 2.8: Seismic Data Sharing

2.4.2 Geological & Geophysical Data Integration

Usually, well data are in depth while seismic data are in time. To view a seismic section with a directional well projected on it, either the seismic needs to be converted to depth or the well converted to time. In both cases, velocity is important to do the conversion. Seismic conversion is a time consuming process and requires a detailed velocity model. Therefore, interpreters prefer to convert wells information into time and tie them to seismic. Most interpretation software provides tools that support such conversion.

Tying well data to seismic helps to find events (seismic reflections) that corresponds to geological formations. There are basically two methods used to tie the geological control into the seismic data: (1) using checkshot data; time-depth pairs, or (2) using synthetic seismogram. The first method is the simplest but least accurate. Because I am not doing a detailed reservoir analyses, I can scarify the quality to use the simplest method (Figure 2.9). This helps me to post the two sands tops on seismic sections at proper times. I posted the checkshot data used in this study at: http://www.geology.uno.edu/GInt/index.html.

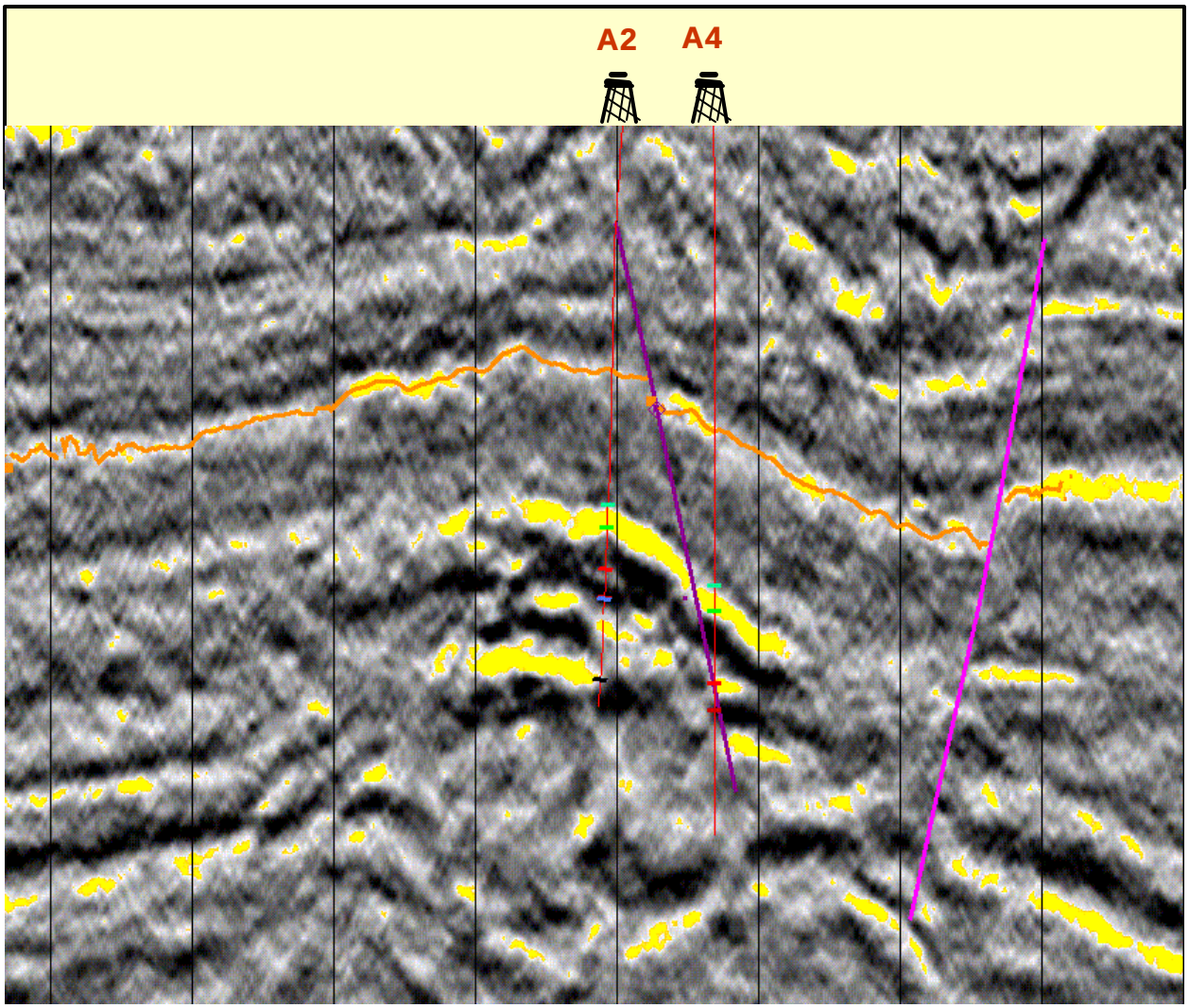

Figure 2.9: Tying well data to seismic with checkshot information

2.4.3 Salt Diapir Picking

Starting with salt picking is a god idea as it is the dominant structure that governs the area. Most other structures are secondary or affected by the salt mobilizations. I found out that salt interpretation is the foundation for any subsequent picking. Usually, picking salt peak is easier than picking salt flank. That is because salt diapirs are gentle at the top and steep at the flanks. Accurate interpretation of salt flanks is very important because many hydrocarbon traps are found at this structural position. Numerous data collection and processing developments have been aimed at this problem (French, 1990). For example, full one-pass 3D migration is considered preferable to the more traditional two-pass approach. Also, collecting the data in a direction strike to the salt/sediment interface will enhance the signal tremendously (Brown, 1999).

2.4.4 Major Faults Picking

Using 3D data to pick faults is tricky. Depending on how you slice the data, a steep fault on one view appears as semi-flat in a different view (Figure 2.10). Thus, a careful interpretation strategy should be followed. In this thesis, I applied the following strategy:

1. Pick any structure that is suspected to be a fault.
2. Validate each picked fault by:

    a. Slicing the seismic in many directions and checking the fault existence.
    b. Trying to find a structural relation ship between the fault and the salt diapir.
3. Assign a recognizable name for each fault that passes the validation step.
4. Interpret one fault at a time using some cross sections with a fixed orientation that best illustrate the fault segment. This should avoid any orientation that is parallel to the fault strike.
5. Use the base map to interpolate between the cross sections interpreted in previous step.

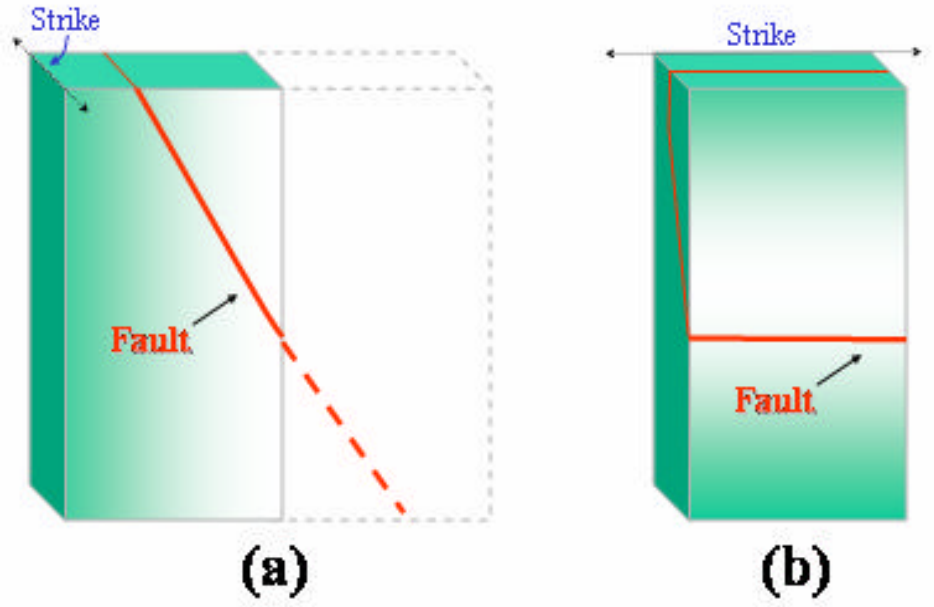

Figure 2.10: Fault representation in 3D. (a) Cross sectional view perpendicular to fault strike. (b) Cross sectional view parallel to fault strike.

2.4.5 Major Sands Picking

The following is an important step every interpreter should take to visualize the area in three dimensions. Some times are needed to set aside and scroll through the seismic in vertical and horizontal orientation in order to get a sense of which direction the structures are trending and where future interpretation problem areas may exist (Tearpock and Bischke, 2003).

In the 3D world, it is impractical to interpret by hand every line, cross-line, time slice, and arbitrary line. To start picking, it is best to begin at well locations

and then work outward from there. Also, it is important to pick within a well defined grid. Not following that, may complicate any interpretation modification.

Horizon interpretations step usually comes after picking the faults. In previous step, I built a pretty good idea about the existing fault types. This helped me in picking horizons and placing proper fault contacts (up or down) whenever horizons intersect fault segments. In this study, I focused mainly on two horizons, which are the top of the 4500-ft and 8500-ft sands, to understand the Pleistocene deposition and relate that to the salt evaluation.

The 4500-ft and 8500-ft sands are very clear events at hydrocarbon accumulations. Figure 2.11 shows both sands on a traverse section. Bright spot and flat spot are illustrated clearly in the figure. The bright spot is presented with high amplitude of negative polarity (yellow color) on the traverse indicating low velocity gas sand. The flat spot, however, is presented with positive amplitude and it is related to gas sand and water sand contact. The flat spot terminates laterally at the same points as does the bright spot. This form of bright and flat spots increased my confidence in sand interpretations and hydrocarbons detections.

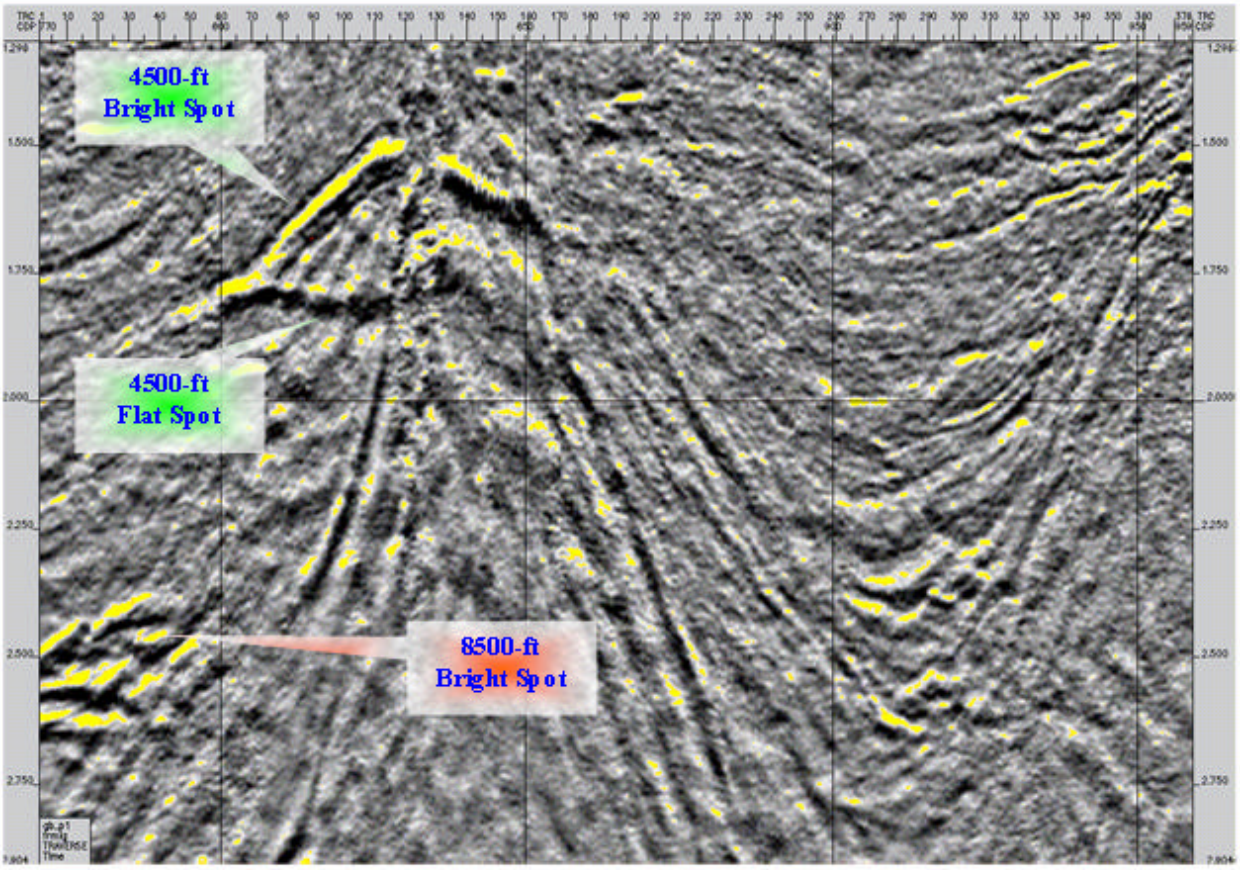

Figure 2.11: Bright and flat spots.

2.4.6 Fault Boundary Creation

A fault trace is a line that represents the intersection of a fault surface and a structural horizon (Tearpock and Bischke, 2003). Two fault traces are normally required to delineate a fault on a structure map (Figure 2.12). IESX refers to these two lines as a fault boundary. In mapping, this practice is used to integrate fault and structure maps.

In this step, I posted fault contacts on IESX *BaseMap* to see the extent and direction of the intersecting faults. Then, IESX *BaseMap* tools were used to crate fault boundaries. This process was applied to one horizon at a time. Every boundary was assigned a fault segment and associated to a specific horizon.

2.4.7 Final Time Map Generation

A wide variety of maps can be obtained from seismic interpretations. Each map presents a specific type of subsurface data extracted from one or more attributes. The purpose of these maps are to present data in a form that can be understood and used to explore for, develop, or evaluate energy resources such as oil and gas.

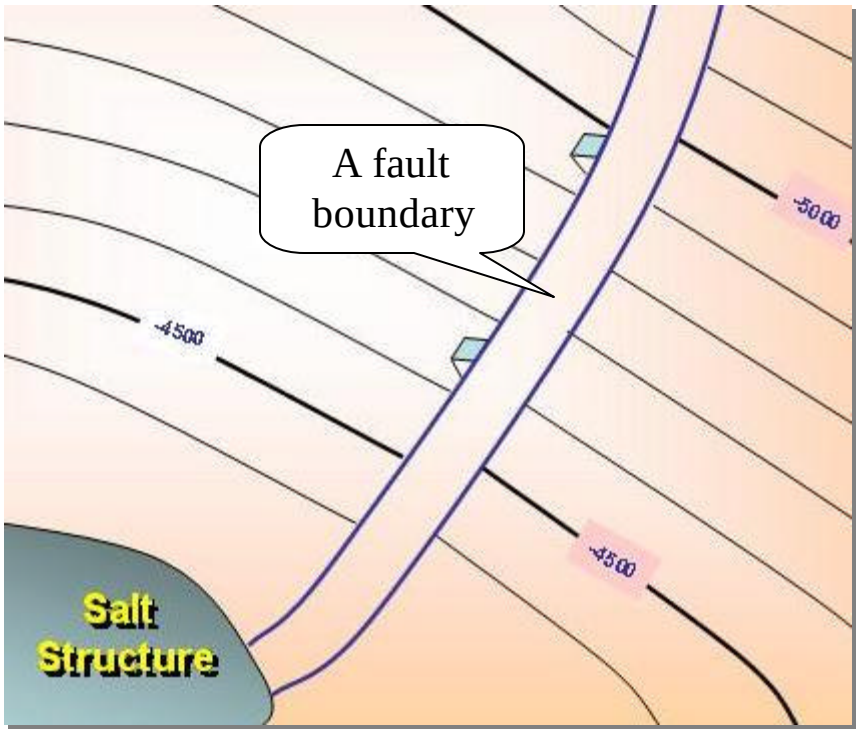

Figure 2.12: Fault boundary example.

The seismic data I used in this study are in time domain. Therefore, the generated interpretations were in time. As I mentioned before, it is not practical to interpret by hand every line and cross-line. So, I utilized an IESX tool, called *ASAP*, to interpolate between the lines. The tool gives options to generate fault contacts where a horizon intersects a fault and not to interpolate within fault boundaries. ASAP picks are flagged and can be deleted at any time without affecting the original picks. Finally, the map was contoured to illustrate surface elevations in two-dimensional view.

2.4.8 Amplitude Anomaly Map Generation

IESX extracts seismic amplitude with every interpretation picks. The tops of 4500-ft and 8500-ft sands, which I picked, are above the reservoir area. To generate amplitude maps that provide valuable stratigraphic and reservoir information, I shifted all interpretation down in time to catch the lowest amplitude that represents the bright spot area. I utilized *Arial Operation* in IESX→*Seis3DV* to do this operation. Final amplitude maps are presented in Chapter 4.

CHAPTER 3: DATA ANALYSIS

A careful study and analysis of data are very important in seismic interpretation. In addition to interpreters' experience, data quality and quantity play a major role in producing acceptable interpretations. Usually, interpreters compete with each other to access additional data with better quality. They look for seismic and seismic related data, well data, and old interpretation and reports. Each datum gives valuable hints to better interpretations. This chapter will go over observations extracted from data utilized in this study and draw a hypothetical view of a subsurface model.

3.1 Observation

We can't depend only on seismic processing to image subsurface structures. Although computers play a major role in imaging, they are not smart enough to fully identify geological formations. We still need human eyes to recognize patterns that computers can't identify. Not only that, human inference is also needed when seismic signals become weak and human eyes loose the pattern. In such situation, interpreters need to do a scientific guess. For such guess, interpreters depend on a general hypothesis based on observations extracted from a careful data analysis and adequate understanding of area geology.

In Garden Banks 191 (GB-191), 4500-ft and 8500-ft sands of Pleistocene deposited during relative lowstand sea level. Sands transported to the area from lowstand deltas to the north of GB-191 (Figure 3.1). The lowstand shelf edge deltas are 10-15 miles to the north of GB-191, where they constitute the main reservoirs at West Cameron 638 and 643 fields (Fugitt. et. al., 2000).

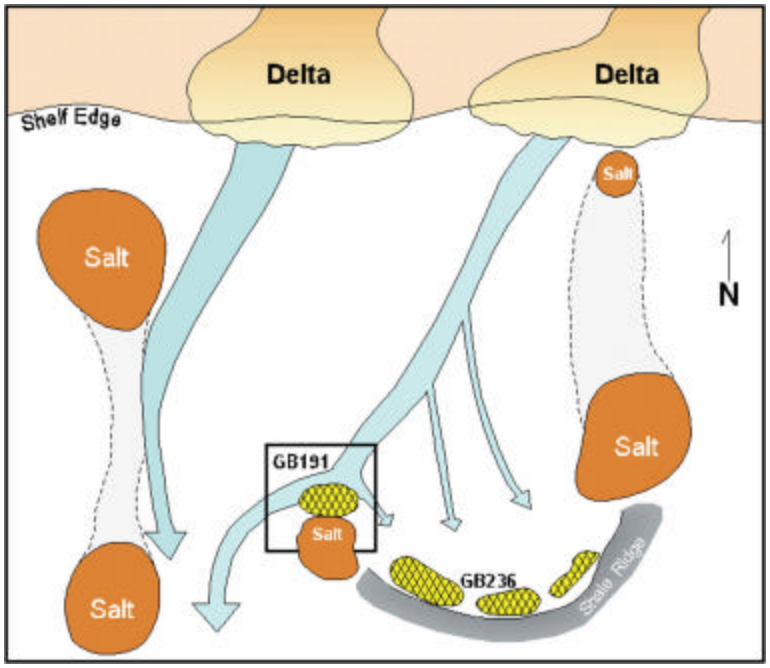

Figure 3.1: Depositional model by Fugitt, Florstedt, Herricks, Wise, Stelting, Schweller, 2000.

After analyzing the seismic data in GB-191 from north to south and from east to west, general observations were obtained. X-lines, cutting the block from north to south, show strata dipping to the north (Figure 3.2). These strata are expected to be deposited during the Cenozoic era on southward dipping slope. This

observation is clear to be identified on X-lines to the left side of the block, where layers are steeper.

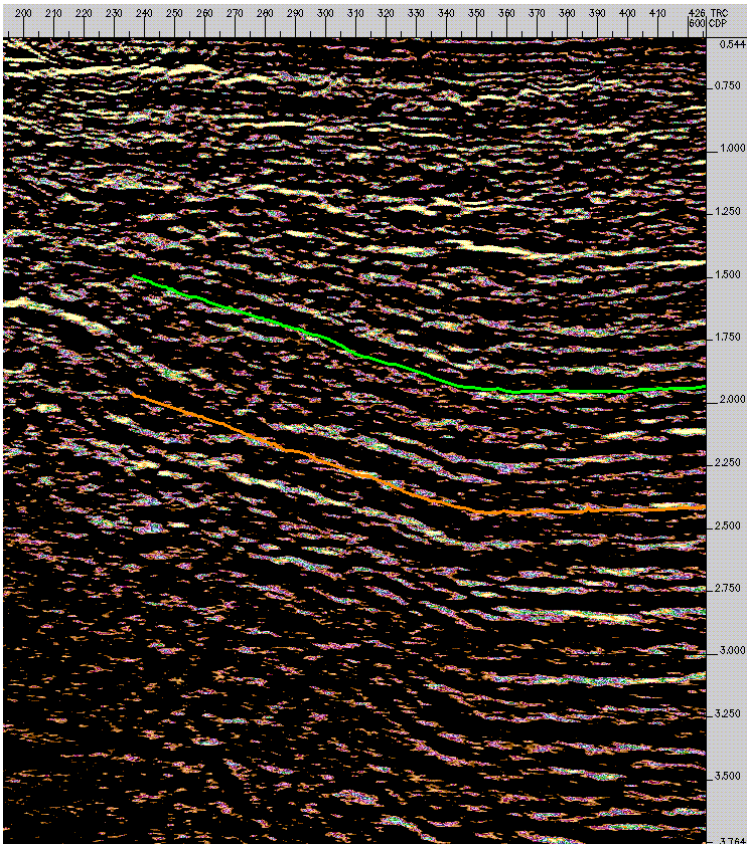

Figure 3.2: *X-line 600*
Horizontal Scale: 1:30,000 Vertical Scale: 2.5 in/sec

Another observation can be identified when In-lines are examined. Figure 4.3 shows seismic reflections to both sides of a salt diaper. Reflections to the left flank reveal steeply dipping strata while they are gentler on the other side. Sands of the same age deposited under similar conditions should match in orientation. This diversity gives a possibility to have some differences in tectonic activity applied on each side of the salt. In general, the overall structure is asymmetric in type.

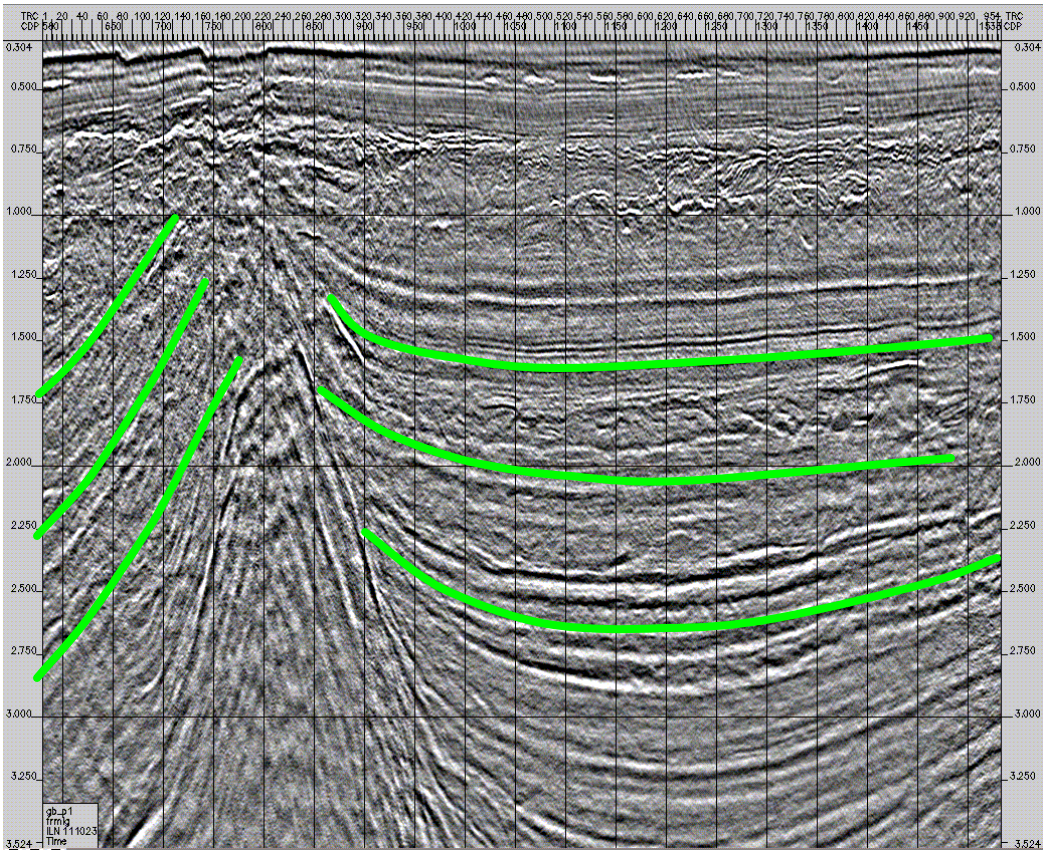

Figure 3.3: *In-line 111023*
Horizontal Scale: 1:60,000 Vertical Scale: 2.5 in/sec.

Faults picking over the same section, shown in previous figure, will enrich our understanding of beds to the west part of the block (Figure 3.4). These beds were uplifted and rotated due to salt diapirism. The change in orientation was accommodated with a series of faults that facilitated the movement. A major normal fault in this series, in purple color, seams to play a significant role in triggering and controlling the shape of the salt structure. This major fault bounded the right side of the upgoing salt body.

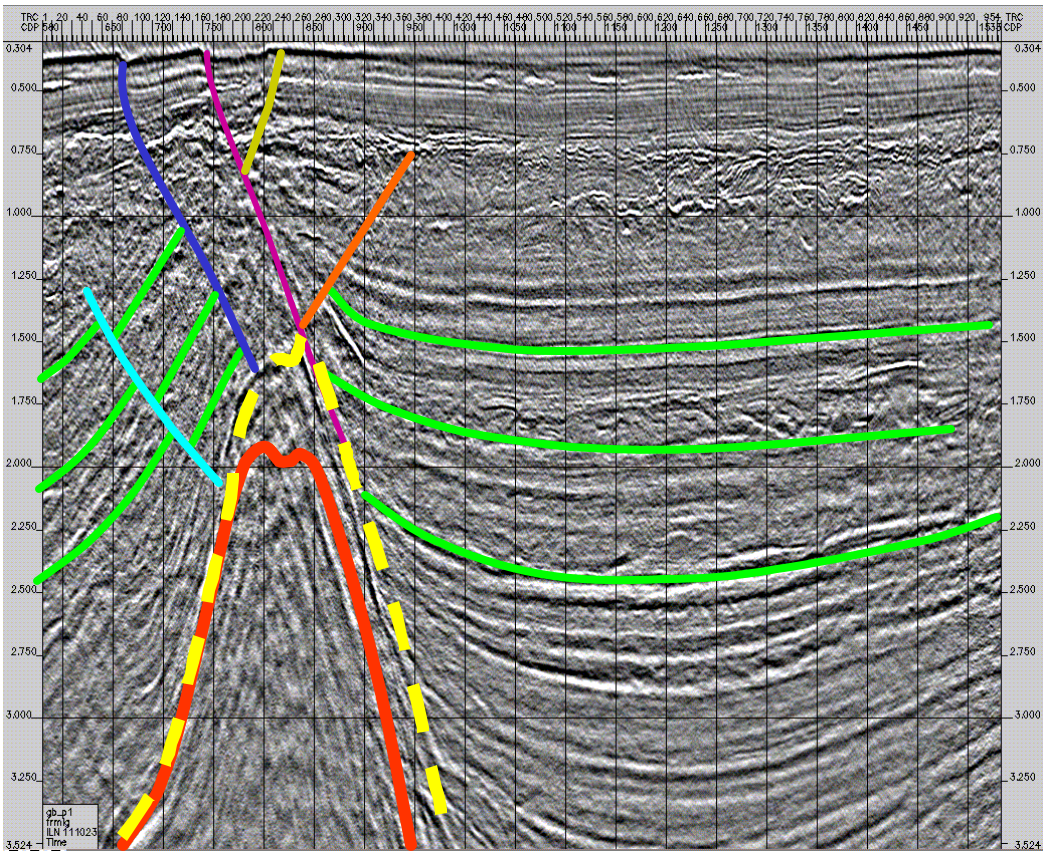

Figure 3.4: *In-line 111023*
Horizontal Scale: 1:60,000 Vertical Scale: 2.5 in/sec.

Dating 4500-ft and 8500-ft sands relative to salt diapirism is an important step in studding GB-191. Seismic reflections, for both sands, show evidence of sediments continuity in prediapiric area. This area is located to the left side of the major fault bounding the salt structure (Figure 3.5). Usually strata in the prediapiric area are uplifted and rotated as salt being added. Therefore, we can conclude that the sands deposition predated the salt diapirism.

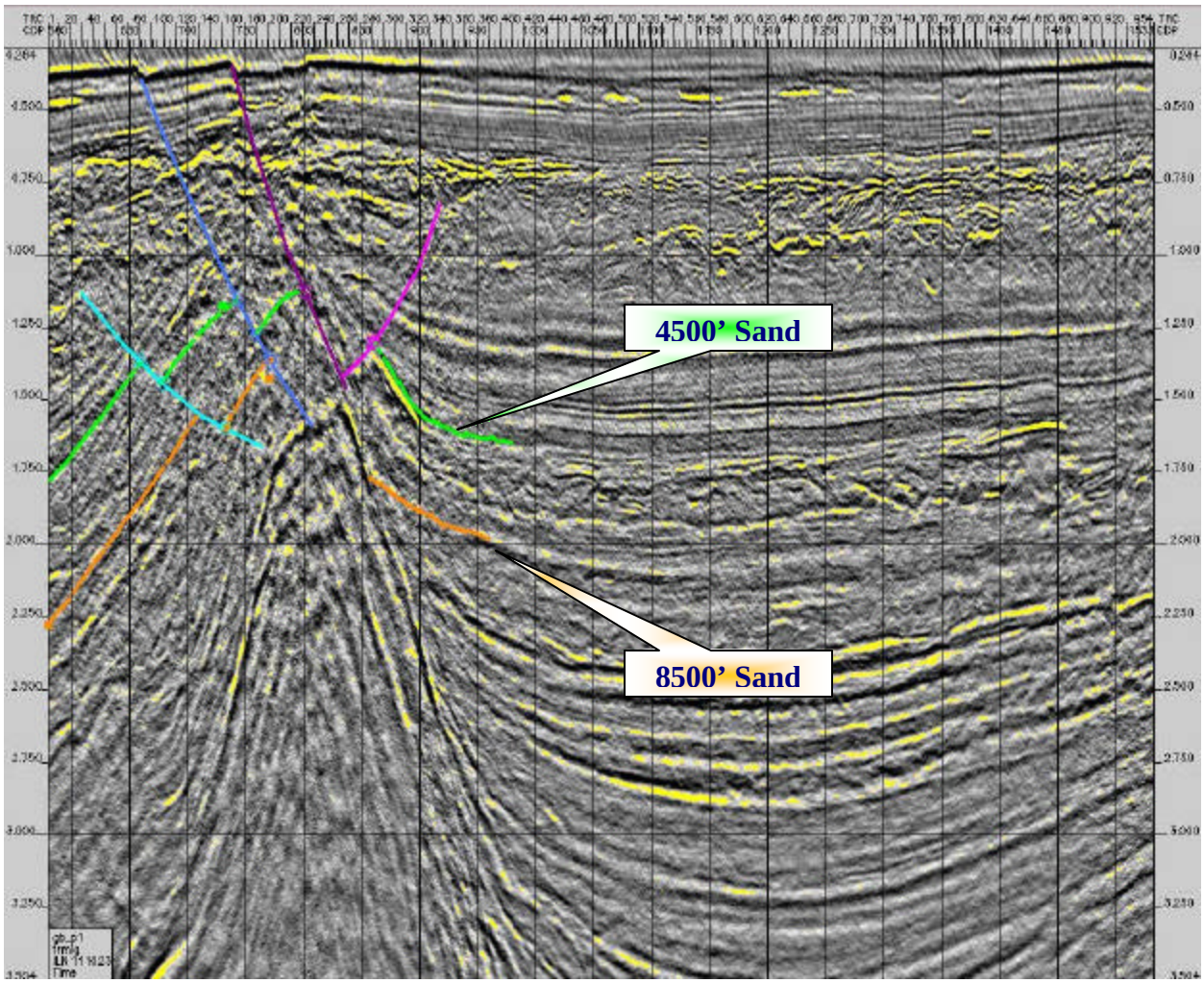

Figure 3.5: *In-line 111023*
Horizontal Scale: 1:60,000 Vertical Scale: 2.5 in/sec.

Additional observation can be seen in picking the salt-upper-limit on some In-line within the block. Figure 3.4 illustrates a challenge by showing two possible limits of the salt. Salt limit, picked in red, is more acceptable over the whole block, while the other is localized in a small area. A potential interpretation of the red limit can be sea-bottom multiples. X-line in the same area can show a different picture (Figure 3.6 X-line 810). The yellow limit is not a continuous event and it is associated with major faults boundaries. Possible shale sheath to both sides of the salt in X-line 810 complicated the picture furthermore. This makes it hard to reach any definite conclusion about the yellow limit.

3.1.1 Observation Summary

The following points summarize the observations explained earlier:

1. Sands of Pleistocene age deposited in GB-191 from lowstand deltas to the north.
2. X-lines from the west part of the block show steeply dipping strata to the north.
3. In-lines from the lower-middle part of the block show asymmetric structure when sediments to the left flank of the salt compared to others adjacent to the right flank.
4. Layers to the west part of the block are steeply dipping northwest and highly faulted.

5. A major bounding fault is on the right flank of the salt dome.

6. 4500-ft and 8500-ft sands exist in the prediapiric area.

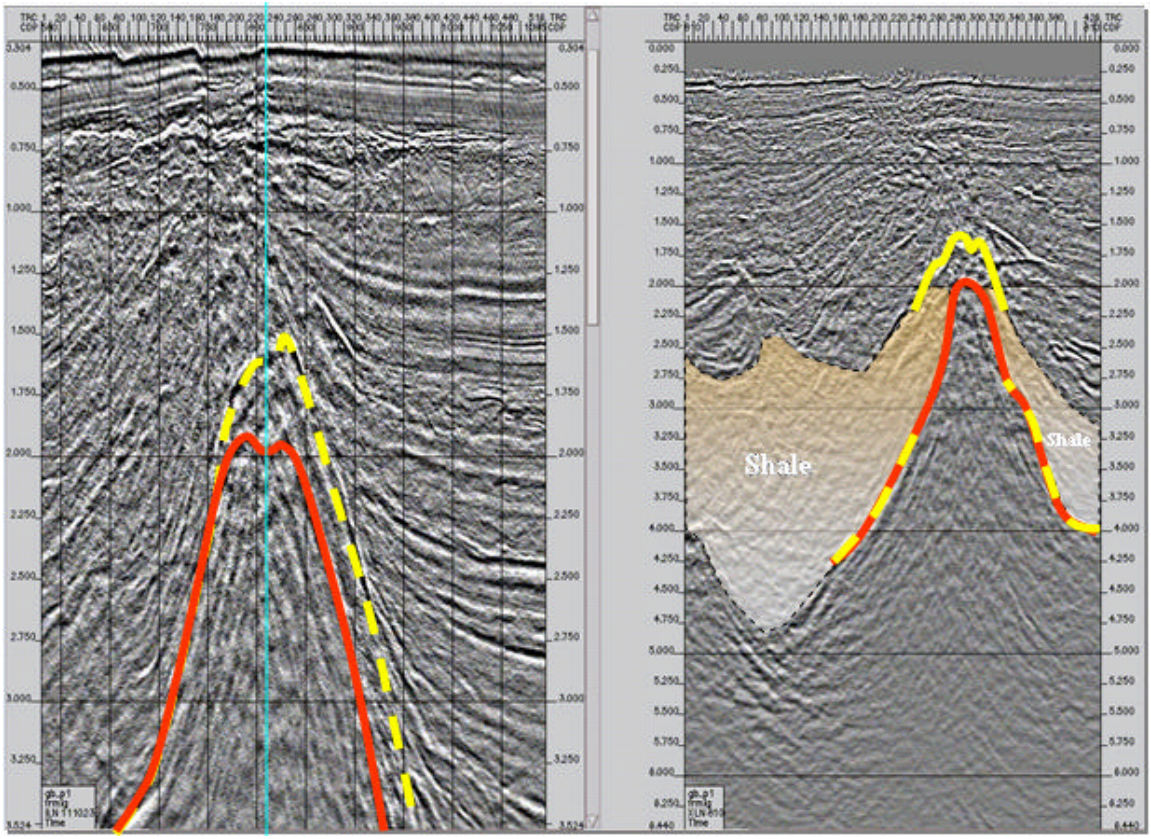

Figure 3.6: *In-line 111023*
Horizontal Scale: 1:60,000
Vertical Scale: 2.5 in/sec

X-line 810
Horizontal Scale: 1:80,000
Vertical Scale: 1.25 in/sec

3.2 Hypothesis

Based on the observations described in previous section, the salt diaper is still in its active stage. The asymmetric nature of the structure and the bounding normal fault are characteristics of active piercement (Nelson, 1991).

In GB-191, the 4500-ft and 8500-ft sands are prediapiric; deposited prior to salt evolution (Figure 3.7a). A major normal fault played a significant role in triggering and/or facilitating the movement (Figure 3.7b). The major fault caused a differential pressure within salt sheet. Structural depression on the downthrown drove salt to migrate upward. Sediments overlaying salt to the left side of the bounding fault were uplifted and rotated (Figure 3.7c). Sediments, however, to the right moved downward as salt was withdrawn from beneath. This process explains the asymmetric structure seen in the area.

In addition to the bounding fault, other secondary faults influenced the salt formation. Couple of faults to the west caused pressure gradient over salt left flank (Figure 3.7d). As a result salts start to migrate upward away from high pressure area.

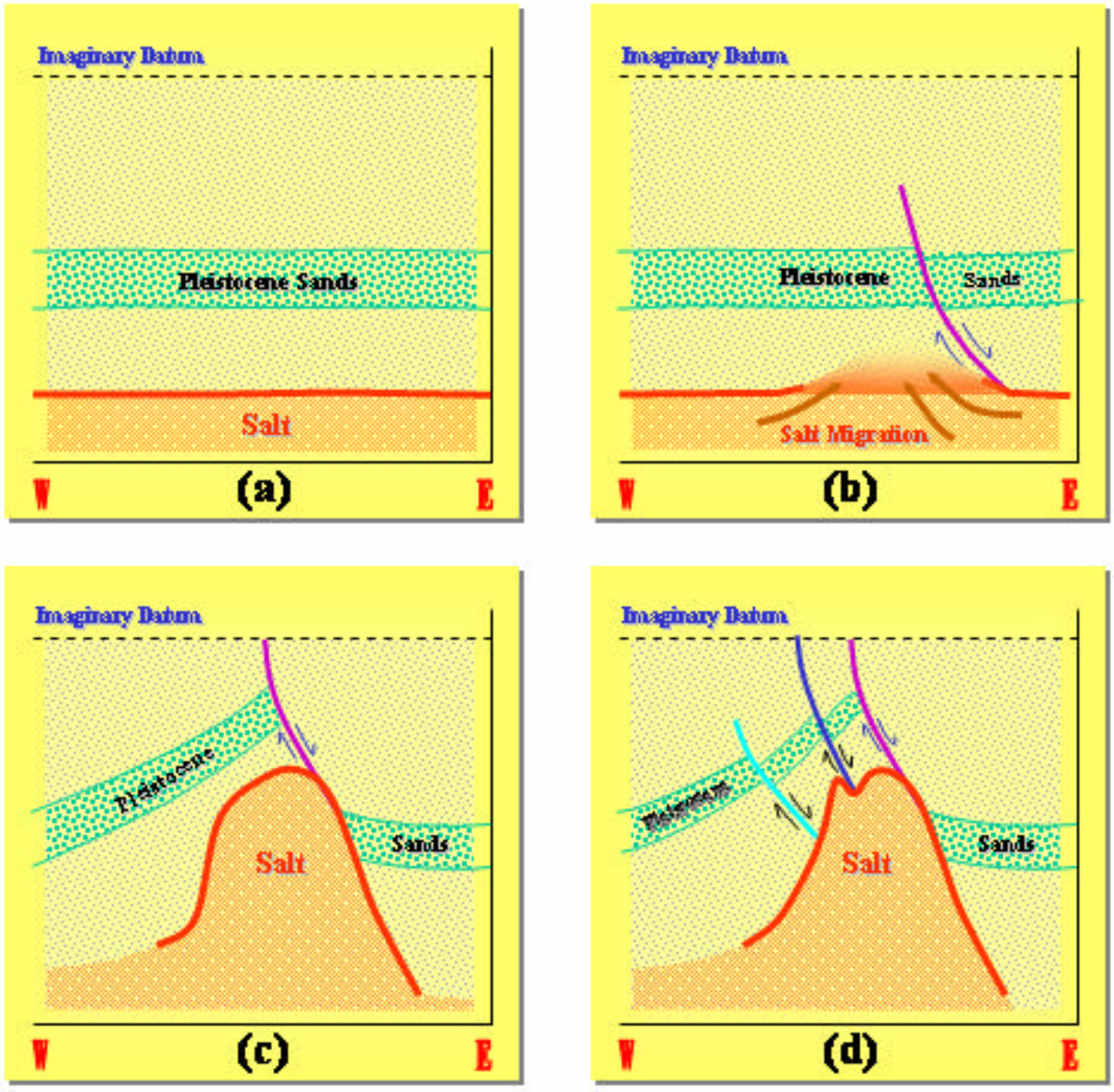

Figure 3.7: Depositional model and salt tectonics. Pleistocene sands predated the salt evaluation (a). Salt migration associated with a bounding fault (b). Salt thrust and uplifted the sands (c). Additional normal faults affected the left flank of the Salt (d).

CHAPTER 4: RESULTS AND DISCUSSIONS

Having a major salt diapir in the middle of GB-191 negatively affected the seismic quality. In some areas, to the west side of the salt, signal resolutions became extremely weak. The thesis hypothesis is important here to map in areas where signal qualities are poor. This chapter will go over thesis results, followed by some discussions, and comparisons to other studies in the same area.

4.1 Structural Interpretation

Geological structures in this field are quite complex and therefore seismic lines require careful examination in order to define main structures. A salt diapir and a set of fault planes are the two main dominant structures in GB-191. The salt diapir is located in the middle-eastern part of the block while fault planes bound the structure.

Salt diapirism split the block into two zones, east and west (Figure 4.1). In the east zone, strata are gently dipping and seismic resolution is superior. This region goes beyond GB-191 to other blocks eastward (GB-192 & 193). The west zone is quite complicated. Strata are rotated, uplifted, and faulted. This makes lateral velocity tremendously vary across the section. Such variations dropped the seismic quality and complicated the interpretation within the area.

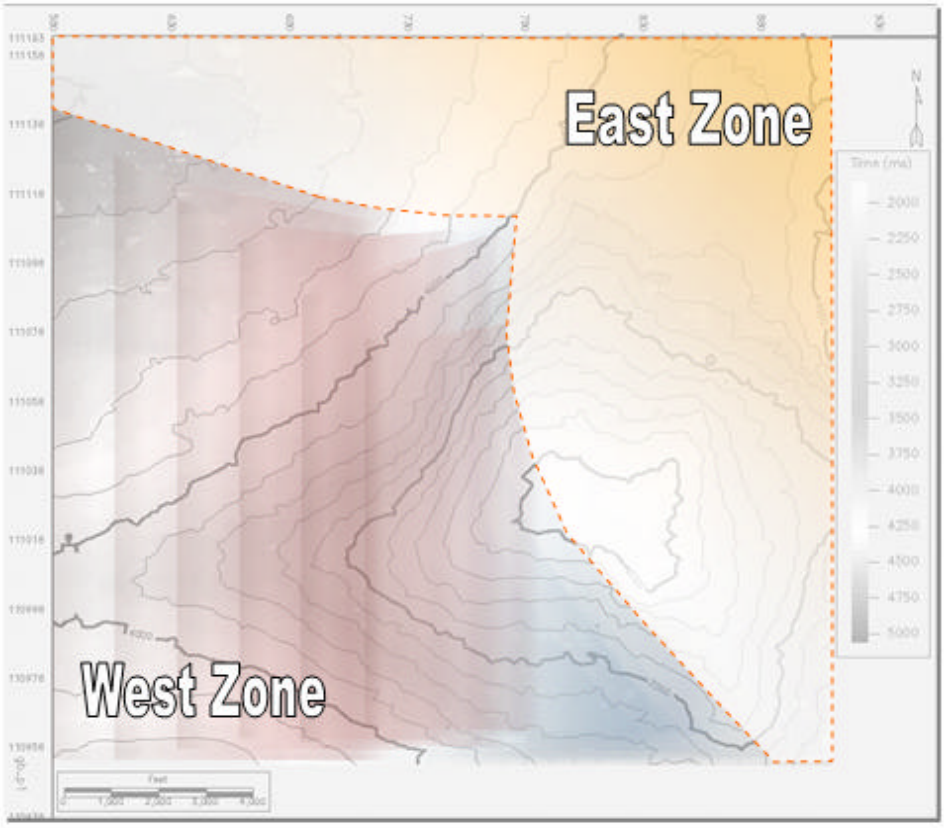

Figure 4.1: Data quality zones posted over the salt map: East Zone is characterized by its smooth reflections, while the other one has more rough signals.

A detailed salt interpretation is illustrated in Figure 4.2. This map view shows the extension of the salt body and its structural peak. By looking at the map view and recalling the thesis hypothesis, we can predict the orientation of overlaying strata. Layers in the west region are steeply dipping northwest, while they are gently dipping on the other side. Salt interpretation on several cross sections is shown in Figures 4.3, 4.4 and 4.5.

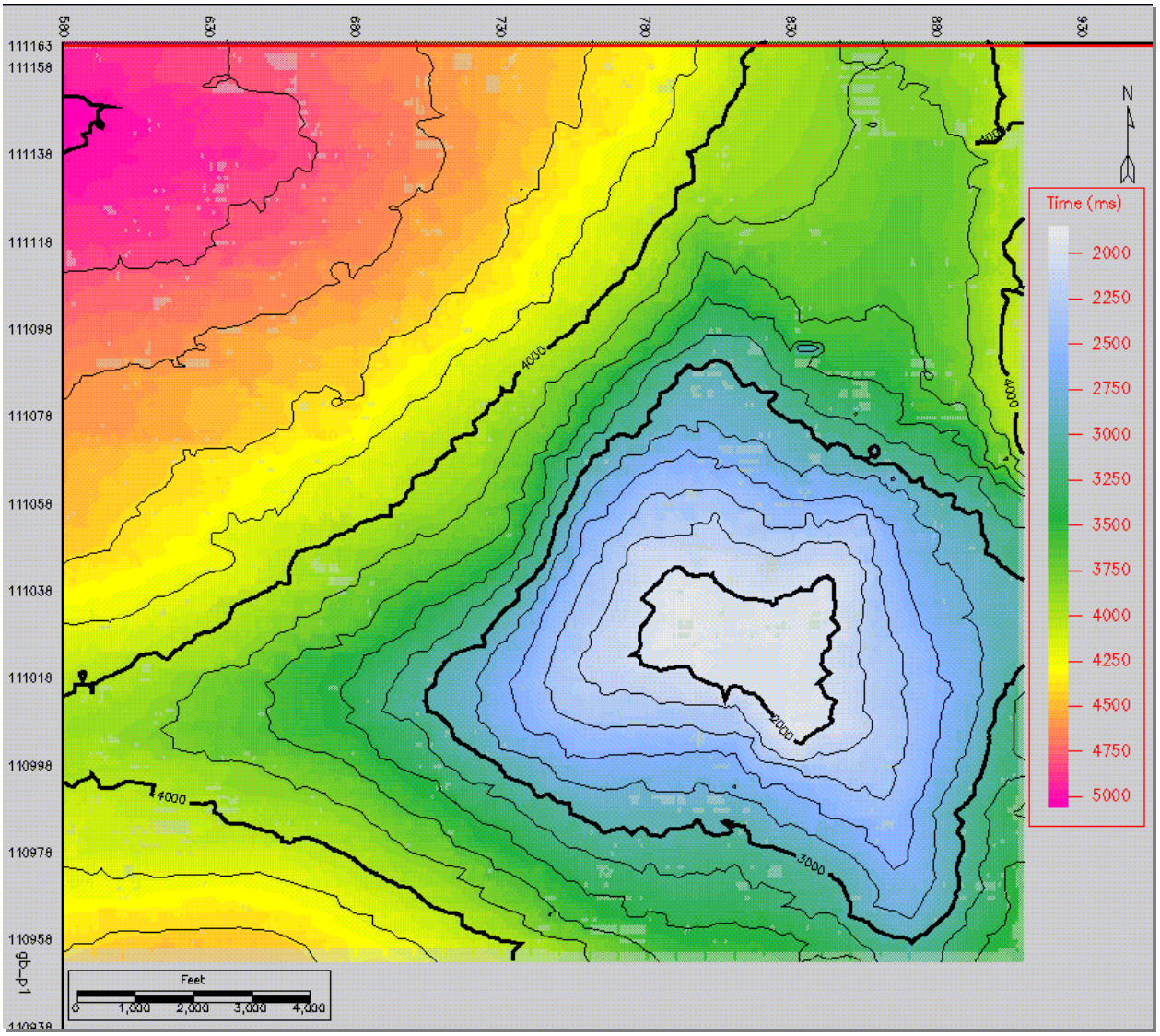

Figure 4.2: Time map of the salt structure. Contour interval is 200ms.

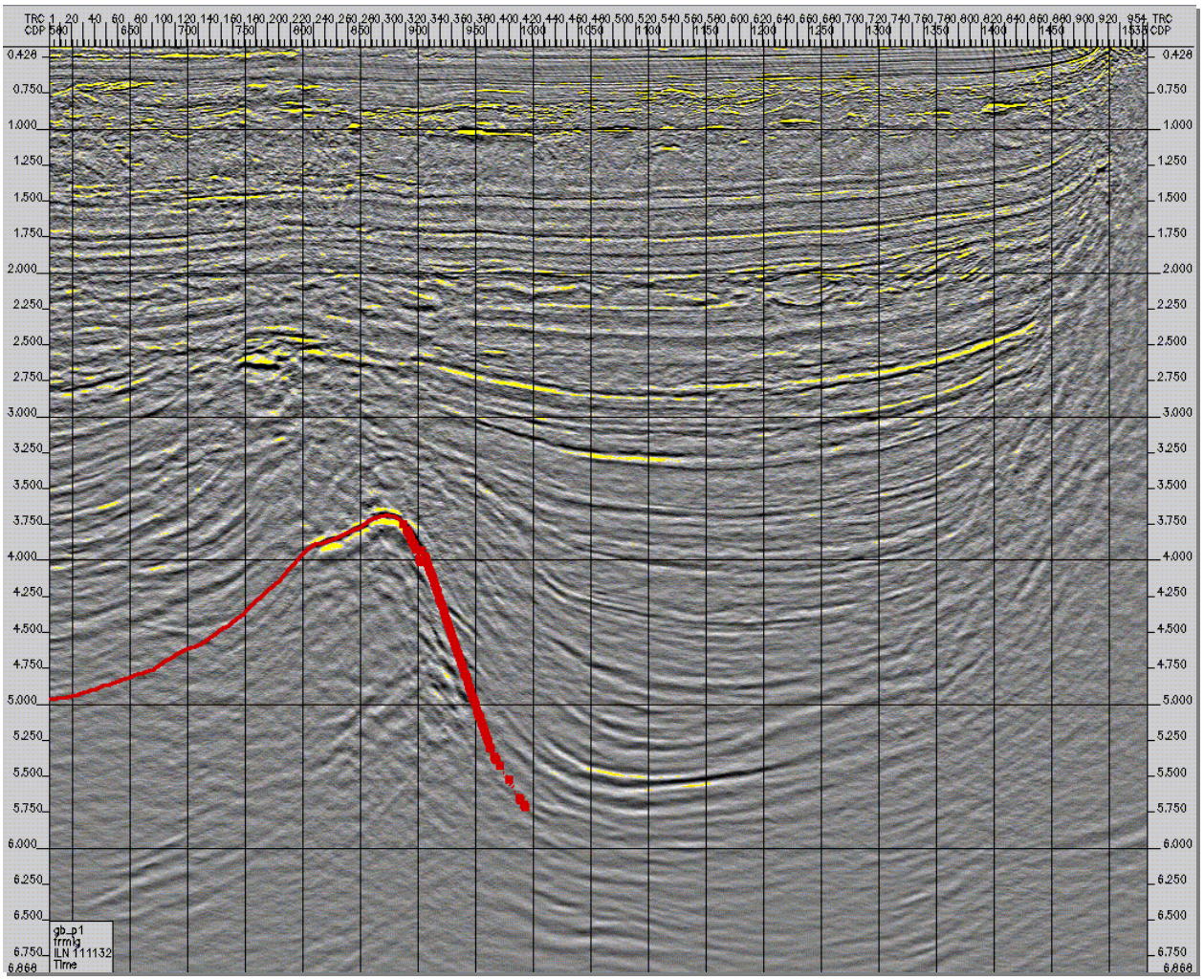

Figure 4.3: *In-line 111132*
Horizontal Scale: 1:60,000 Vertical Scale: 2.5 in/sec.

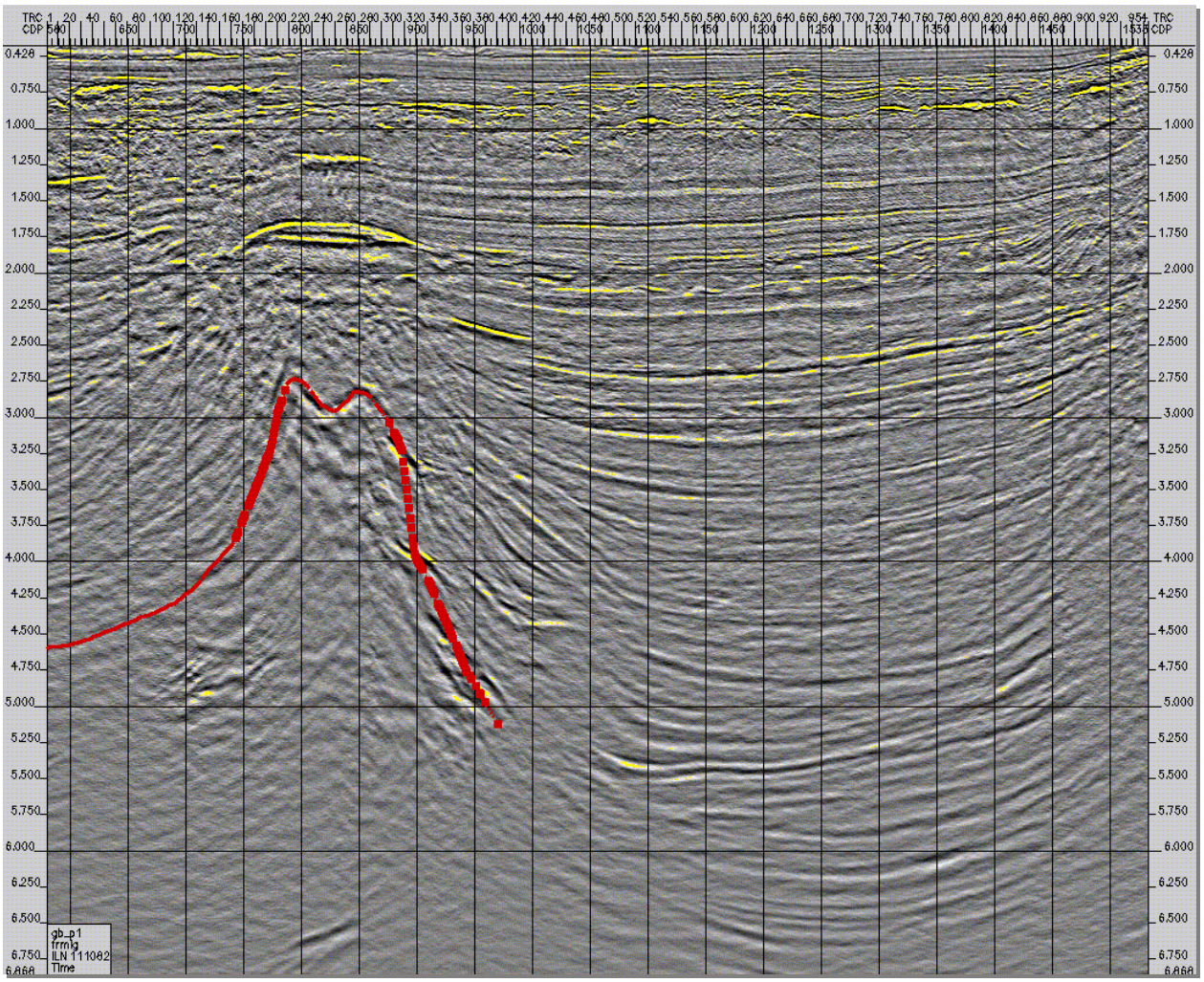

Figure 4.4: *In-line 111082*
Horizontal Scale: 1:60,000 Vertical Scale: 2.5 in/sec.

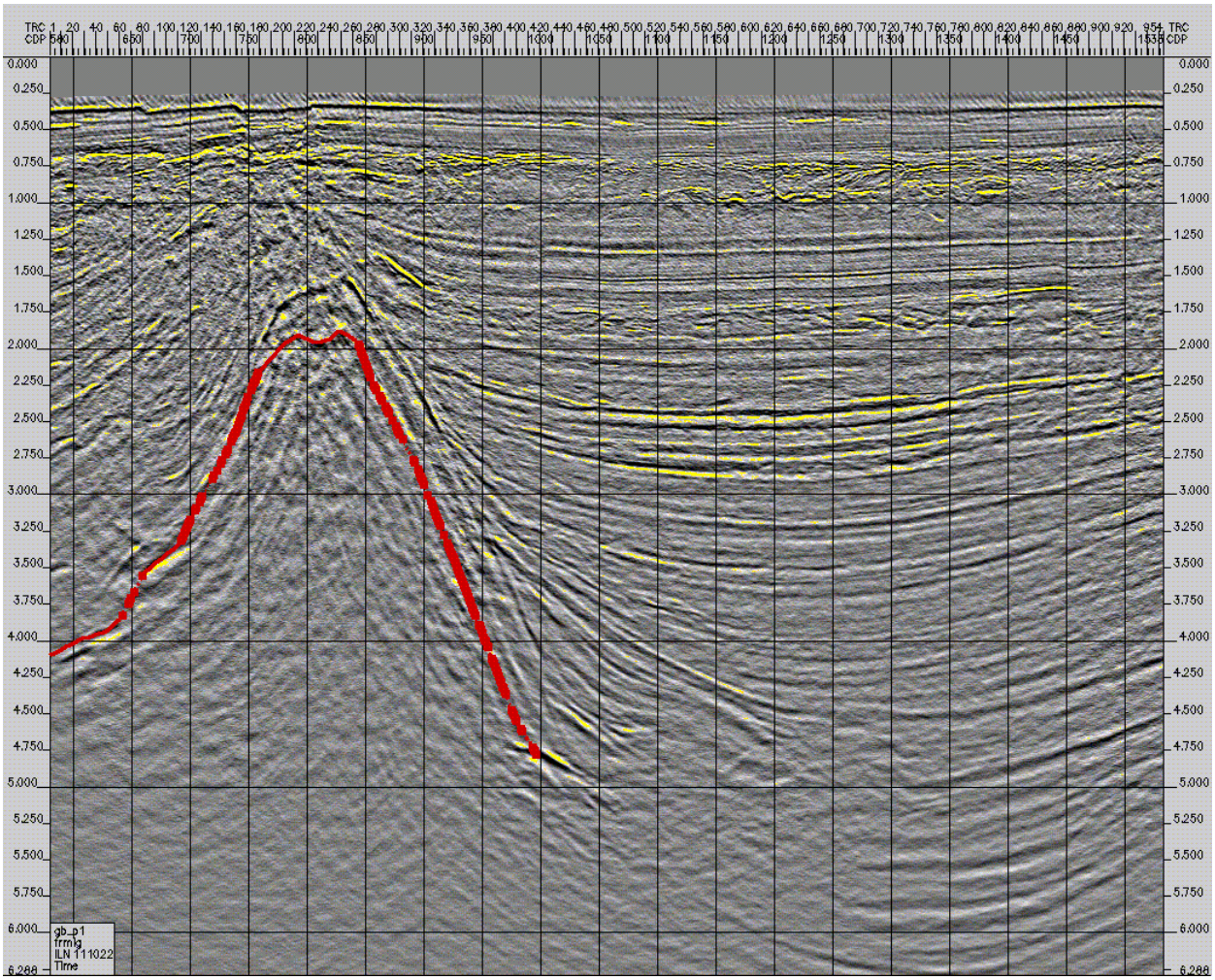

Figure 4.5: *In-line 111022*
Horizontal Scale: 1:50,000 Vertical Scale: 1.5 in/sec.

Fault is the other structure element in GB-191. Usually, faults are picked by tracing bulk signal termination. Every interpreter has his own way to detect such termination. Personally, I prefer vertical exaggeration to search for vertical shifts. Figure 4.6 illustrates the beauty of exaggeration in pronouncing fault structures.

In GB-191, there are five major normal faults planes (Figure 4.7). A bounding fault, mentioned in previous chapter, is the dominant fault that controls the overall structure (shown in purple). Actually, it is a physical border between the east and west zones. Strata in the east zone (fault downthrown) are slightly modified and pierced by the salt. In contrast, strata in the west zone (upthrown) are uplifted and rotated but not pierced by the salt.

Figure 4.7 shows another fault (pink color) that intersects with the bounding fault. Such structure is referred to as compensating faulting. Usually, this type of structure creates garben and horst system. A close image for the system is shown in Figure 4.8.

Other faults in GB-191 are located to the left of the bounding fault in the west zone. Tracing these faults over all seismic sections is challenging. As I mentioned, data quality is poor in this zone. Therefore, fault locations were picked over good reflections and estimated over the week ones. In general, these faults accommodated the uplift in strata within the region. As a result, they reduced the

tension within the uplifted strata and introduced a new pressure over the salt-west-flank.

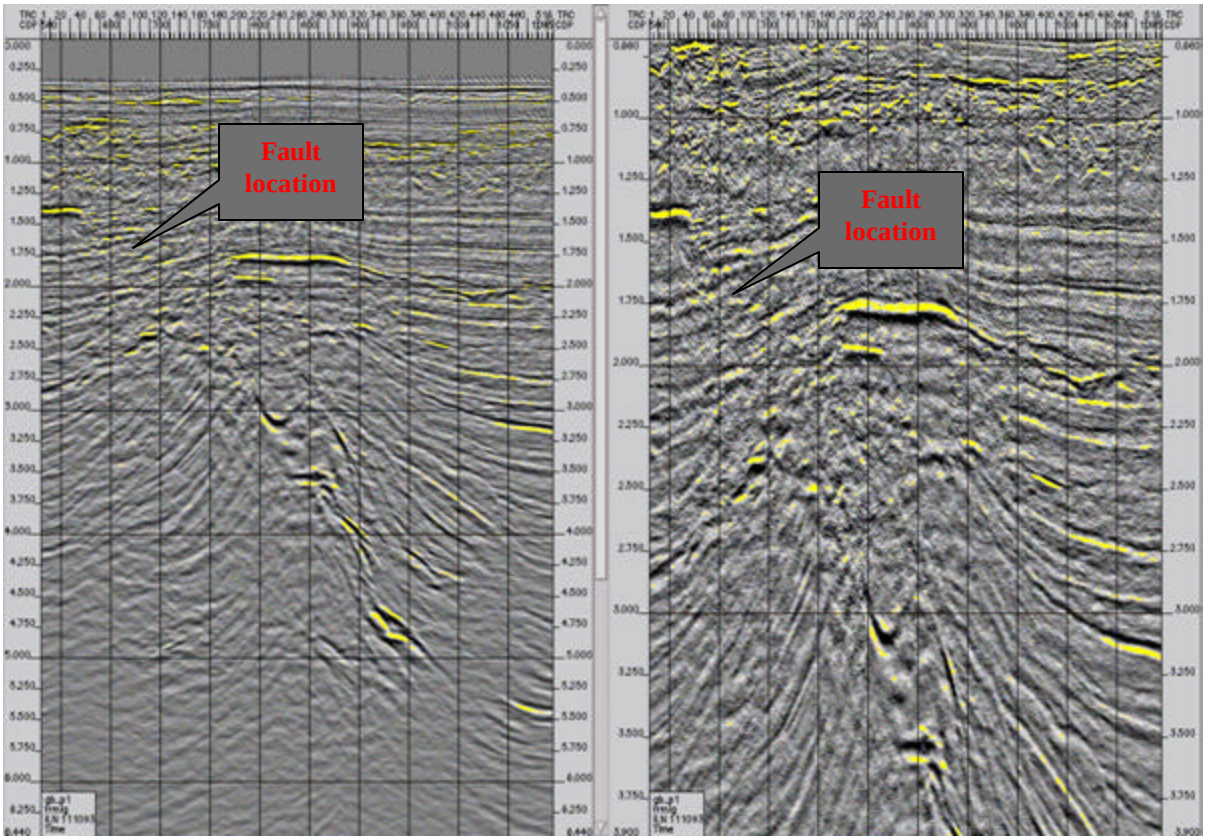

Figure 4.6: *In-line 111093*
Horizontal Scale: 1:50,000 Horizontal Scale: 1:50,000
Vertical Scale: 1.5 in/sec. Vertical Scale: 2.5 in/sec.

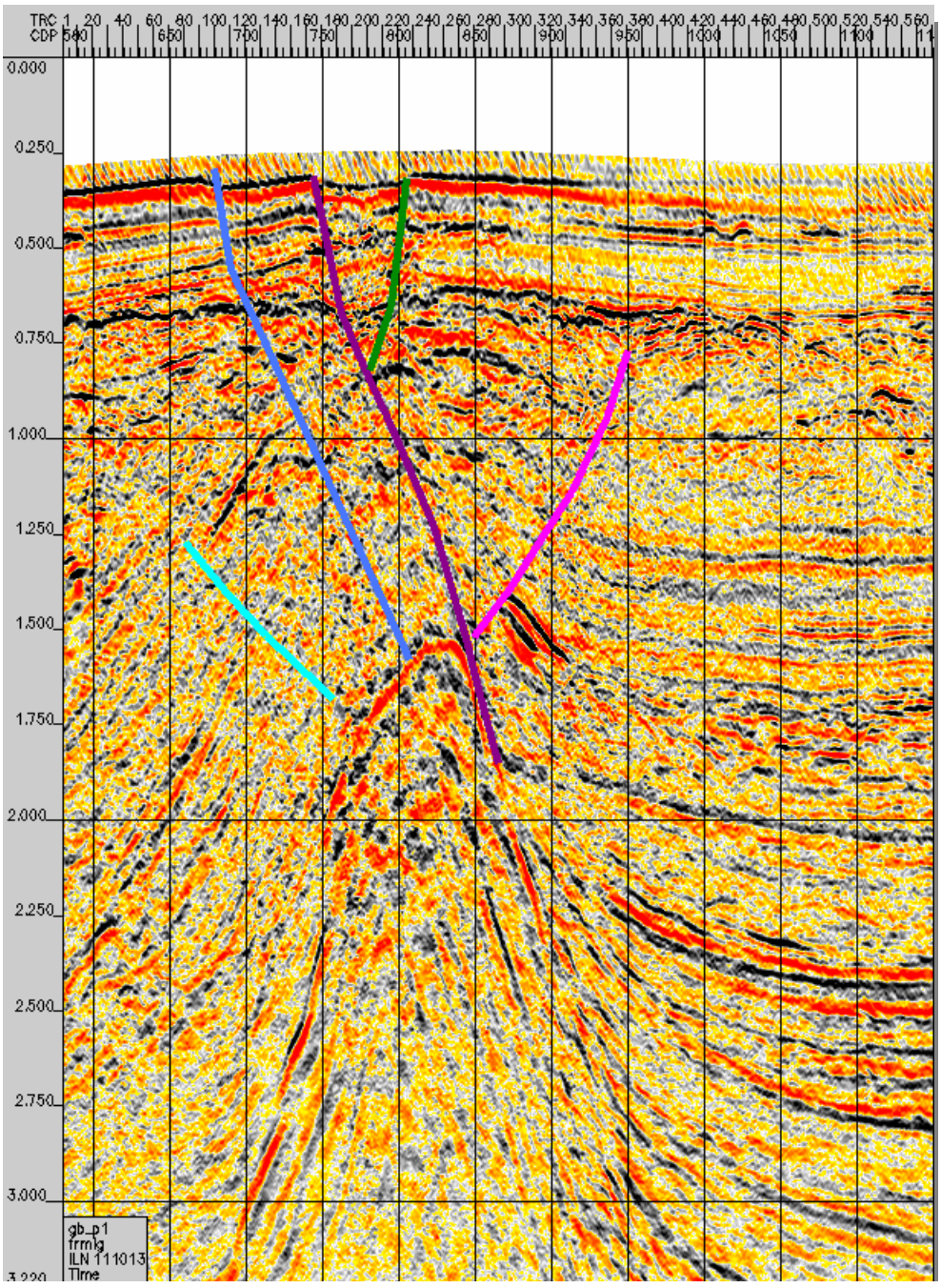

Figure 4.7: *In-line 111013*
Horizontal Scale: 1:60,000 Vertical Scale: 2.5 in/sec.

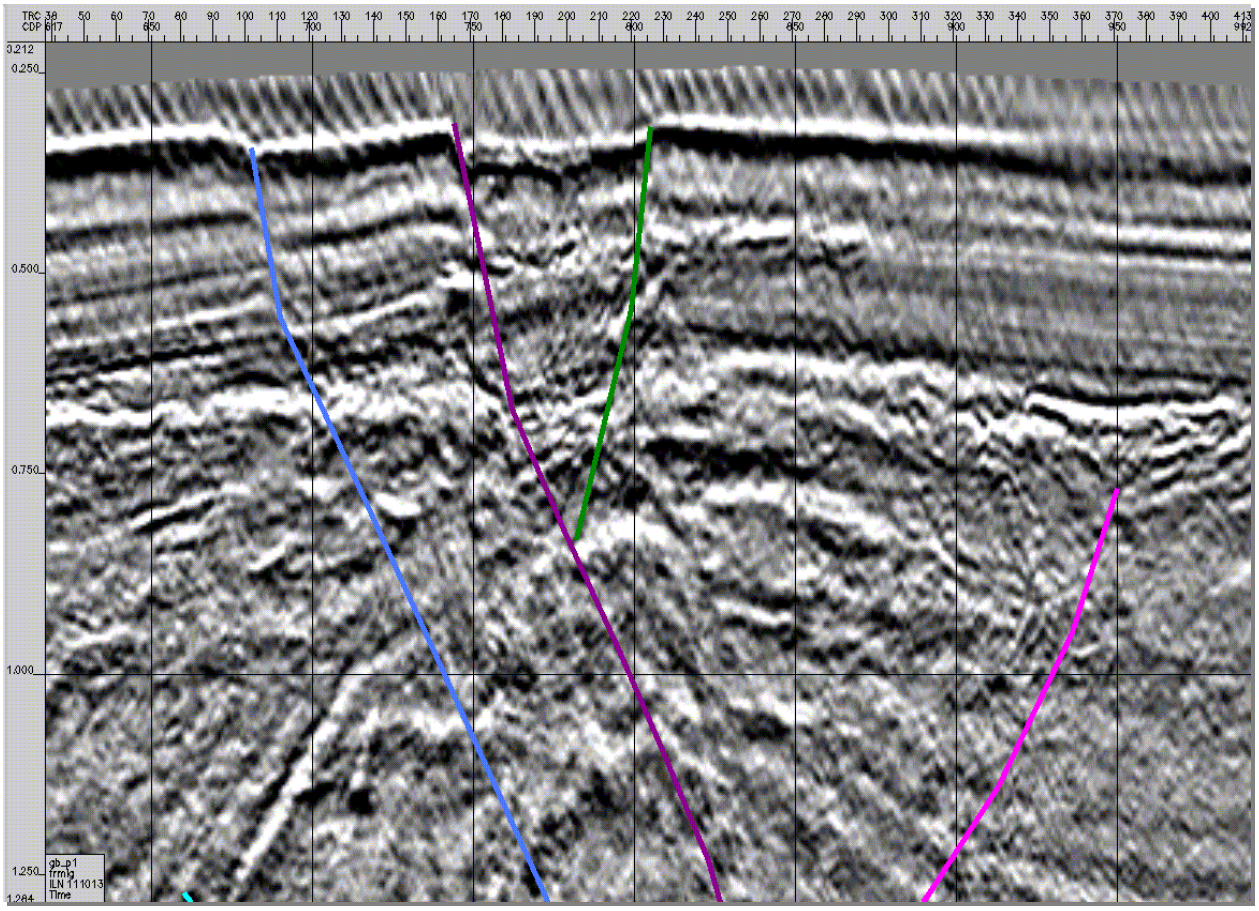

Figure 4.8: *In-line 111013*
Horizontal Scale: 1:30,000 Vertical Scale: 5.0 in/sec.

4.2 Stratigraphical Interpretation

Well markers were used to identify both sands reflections (4500-ft and 8500-ft) over the seismic. These markers were generated from the geological interpretation process explained in chapter 2. Then, seismic interpretations were carried on from well locations to other parts within the block.

4.2.1 The 4500-ft Sand

Figure 4.9 shows a time map for the top of 4500-ft sand. As expected, the layer is steeply dipping northwest in the west zone, which is to the left of the bounding fault. Tracing the sand in this zone was quite challenging. I couldn't use X-lines to track the sand from north to south within the zone. Instead I used some composite lines that go through the east zone, where data quality is better, and then continue south in the west zone.

The 4500-ft sand has a high vertical resolution over seismic sections within GB-191. This is related to its physical thickness, which is about 1000ft. The sand has four members divided by thick shale lamination throughout the reservoir area (Fugitt. et. al., 2000). This limits its vertical permeability and makes every member act as a separate tank during production. The reservoir produced more than 87 billion ft^3 of gas since first production in June 1994 (Fugitt. et. al., 2000).

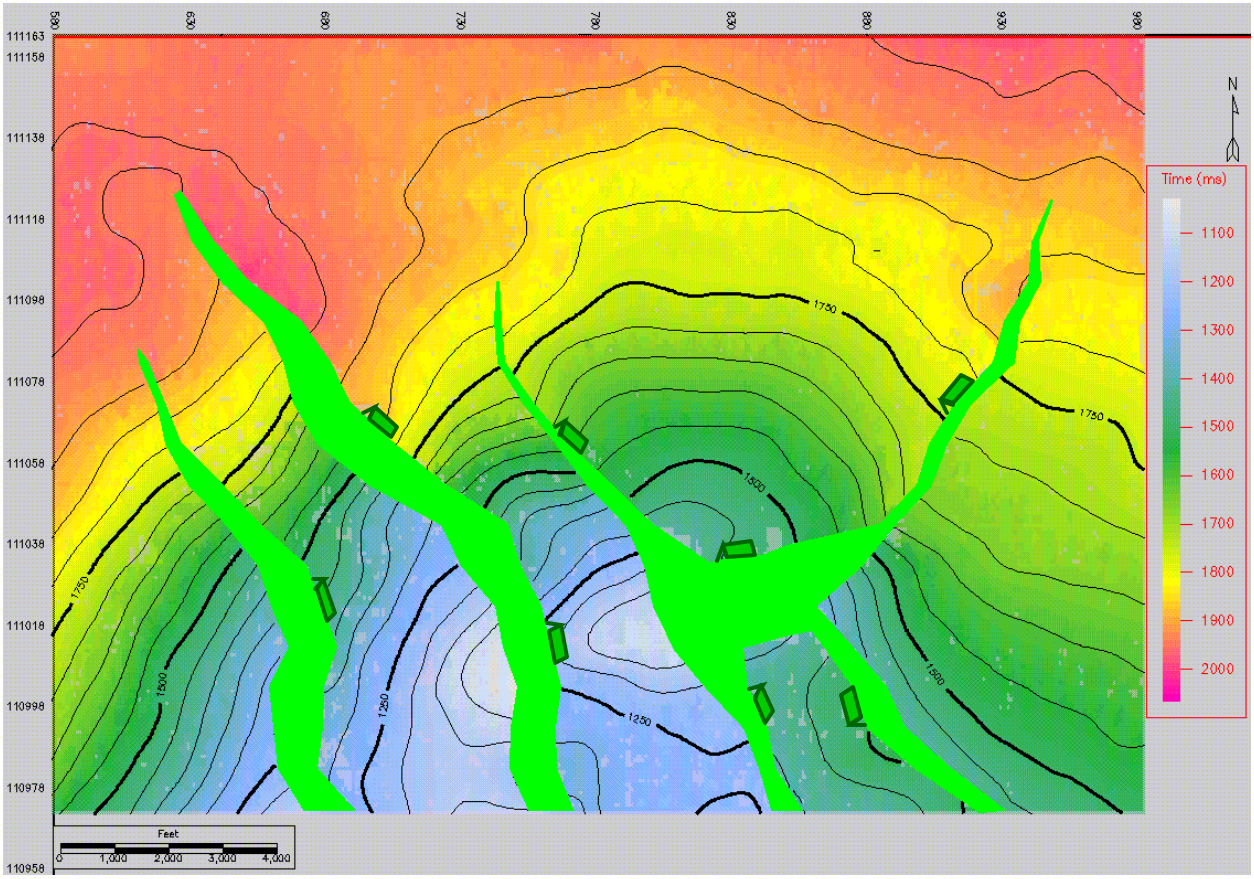

Figure 4.9: Time map for the 4500-ft sand. Contour interval is 50ms.

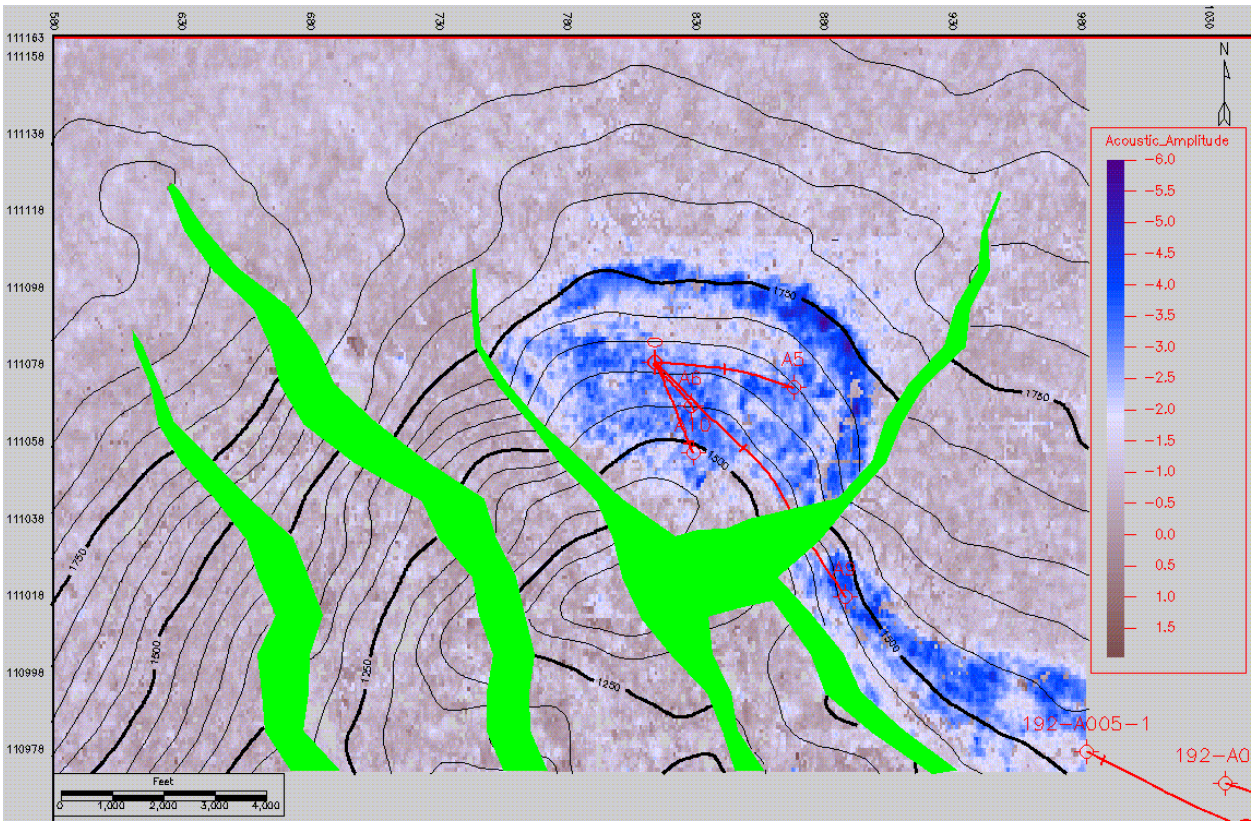

Figure 4.10: Amplitude map of the 4500-ft sand. Time map contours are superimposed.

Figure 4.10 shows an amplitude map for the 4500-ft sand. There are two areas with low amplitudes indicating a possibility of hydrocarbon existence. The area in the middle of the block is trapped by faults from the east, west, and south. Three major wells drilled (A5, A6 and A10) in this area. These wells produced about 97 billion ft^3 of gas. The other area is located to the right bottom corner of the block. A9 is the only deviated well drilled from the GB-191 platform targeting this area. Another well (192-A005-1), shown on the map, hit the area within GB-192 limit. A9 produced only 6 billion ft^3. 192-A005-1, however, produced 7 more billion ft^3 since first production in 1988. Table 4.1, 4.2 and Figure 4.11 summarize production history.

Table 4.1: Gas production in MCF for the 4500-ft sand within GB-191 (calculated from MMS data).

Well Name	A005	A006	A009	A010
API Number	608074012800	608074013200	608074012900	608074064700
1994	--	8338103	220567	--
1995	1920037	20405580	2741231	--
1996	18709734	11091237	1836481	--
1997	14473339	2213037	1021226	--
1998	873936	6563549	277786	134234
1999	475	4732156	356	1771979
2000	0	2383368	0	1049870
2001	0	659107	0	1113863
2002	0	0	0	705997
2003	0	0	0	42227
2004	0	0	0	0
Total	35977521	56386137	6097647	4818170

Table 4.2: Gas production in MCF for the 4500-ft sand within GB-192 (calculated from MMS data).

Well Name	A05-1
API Number	608074002001
1988	565275
1989	2235587
1990	2853967
1991	2415520
1992	2087965
1993	2238560
1994	1130027
1995	0
Total	13526901

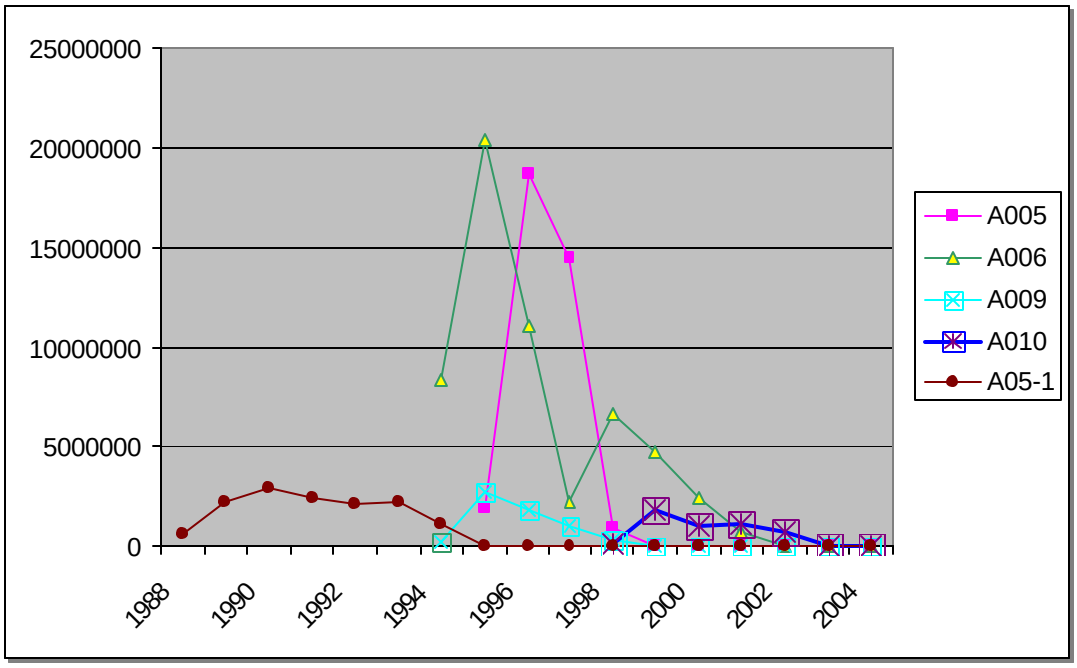

Figure 4.11: Production history in MCF for the 4500-ft sand.

4.2.2 The 8500-ft Sand

The 8500-ft sand doesn't have clear reflections over seismic. In areas where sand is saturated with gas, I was able to identify the layer but without tracing distinctive seismic signals. Therefore, I utilize a phantom, above the sand, that mimics the targeted geological surface in order to map the top of the 8500-ft sand (Figures 4.12 and 4.13). Mapping result is presented in Figure 4.14.

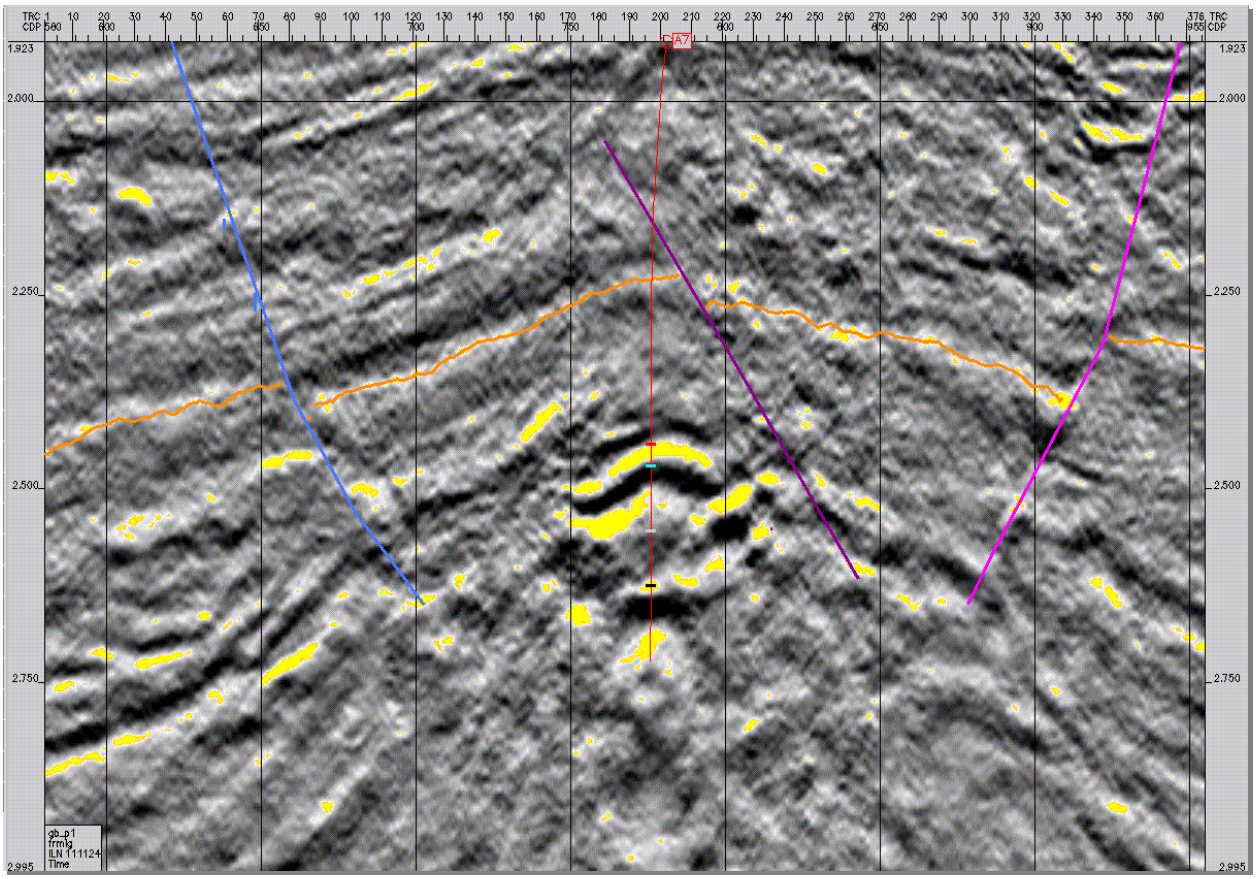

Figure 4.12: *In-line 111124*
Horizontal Scale: 1:20,000 Vertical Scale: 7.5 in/sec.

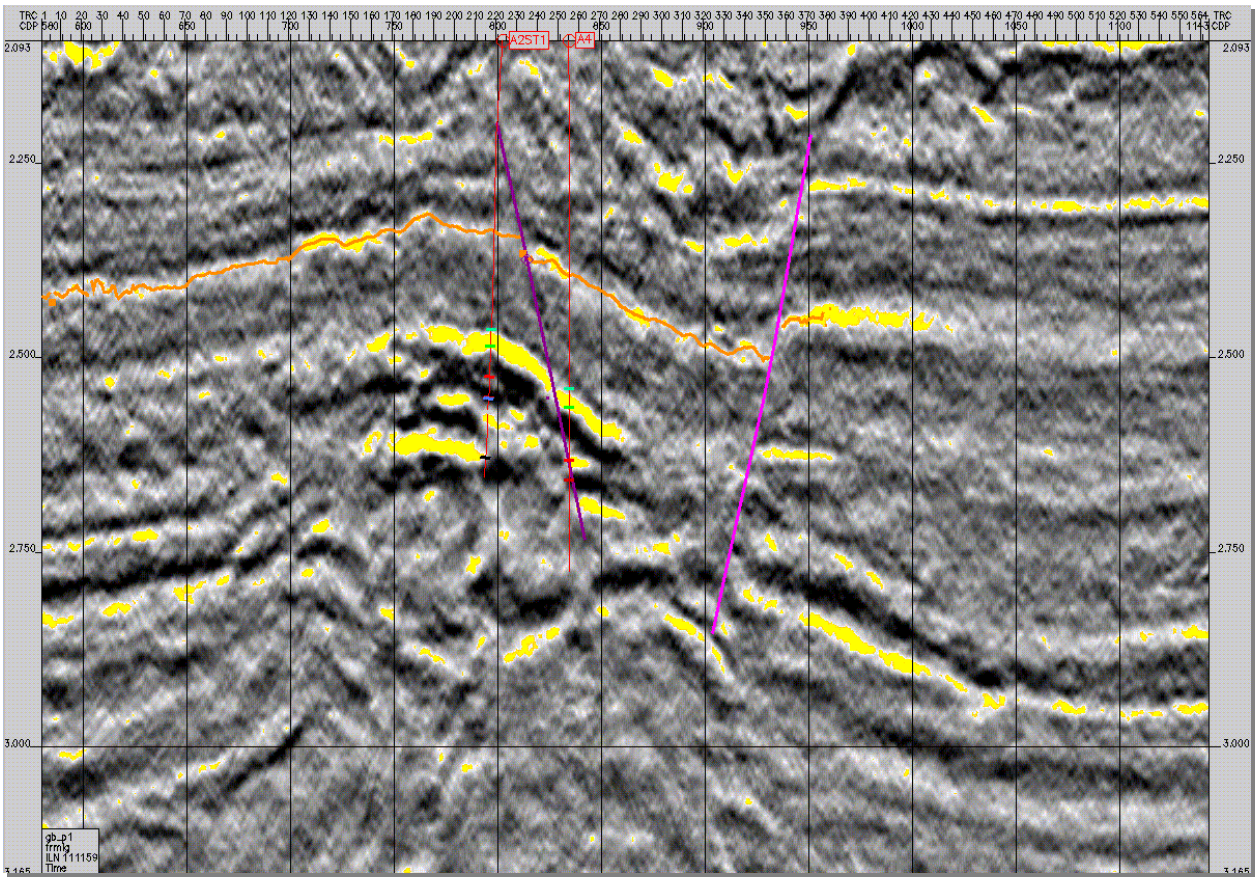

Figure 4.13: *In-line 111159*
Horizontal Scale: 1:40,000 Vertical Scale: 7.5 in/sec.

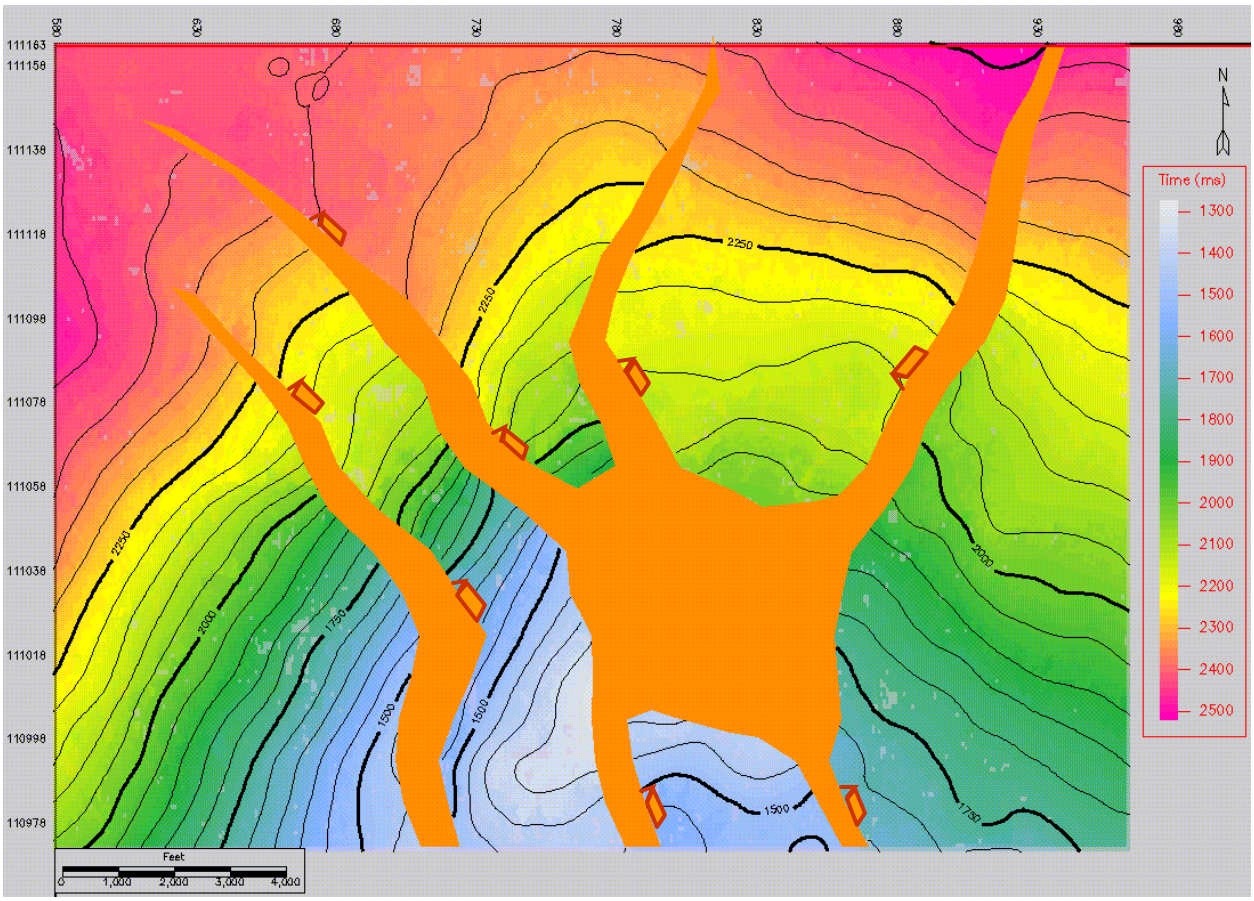

Figure 4.14: Time map for the 8500-ft sand. Contour interval is 50ms.

The 8500-ft sand is 900 ft thick. It is divided into five members separated by shale sheets (Fugitt. et. al., 2000). The divisions were based on geology and were to facilitate reserve estimation. The sand has good vertical connectivity but poorer lateral connectivity. The vertical connectivity allowed the 8500-ft sand to act as a single tank and allowed the existing wells to effectively drain the gas reserves (Fugitt. et. al., 2000).

Amplitude map gives an idea on the extent of the reservoir (Figure 4.15). Three wells drilled to target different parts of the reservoir within GB-191. A7 is the latest one to drill in 1998. It produced 2 billion ft^3 of gas. The other two wells started the production in 1994 and 1995. The initial production rate of the three wells has declined steadily through time and finally depleted (Table 4.3 and Figure 4.16).

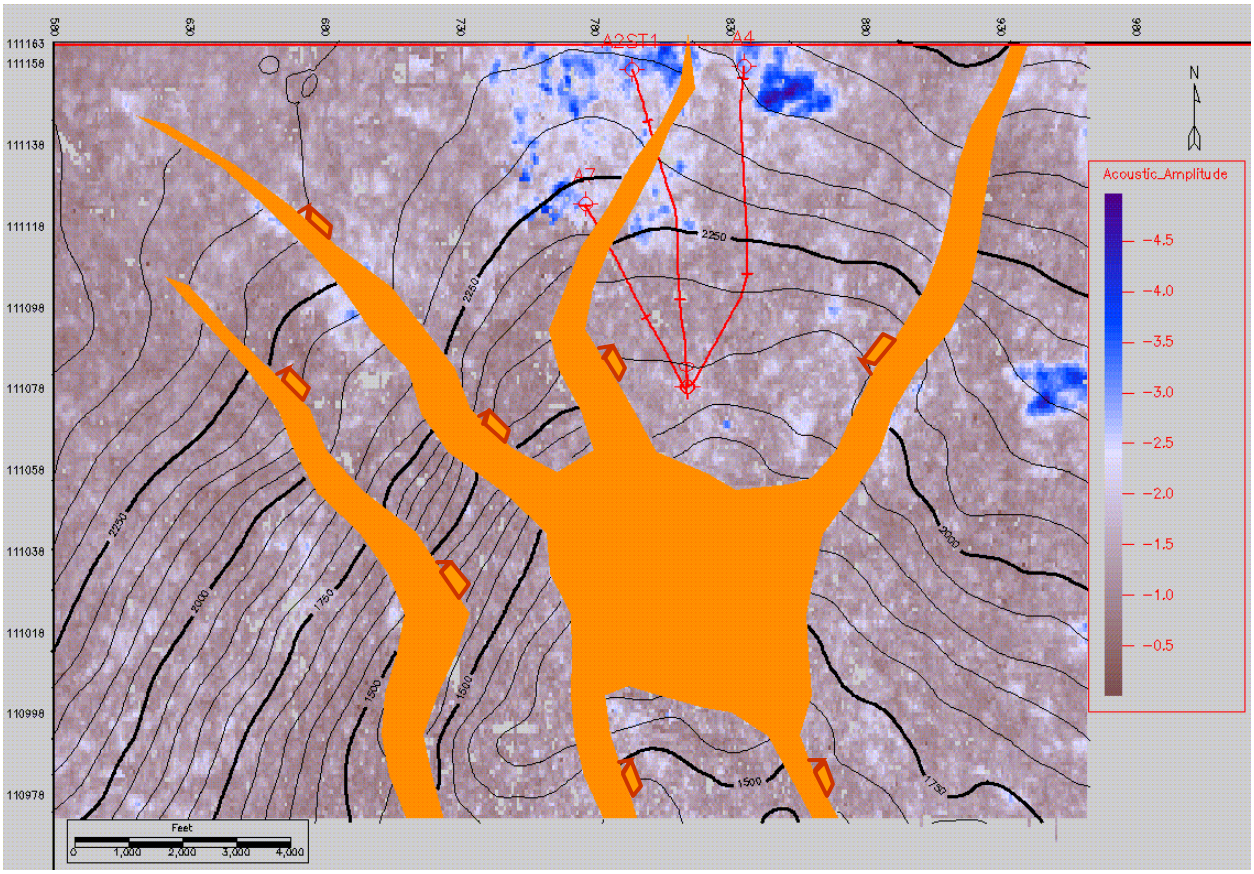

Figure 4.15: Amplitude map of the 8500-ft sand. Time map contours are superimposed.

Table 4.3: Gas production in MCF for the 8500-ft sand within GB-191 (calculated from MMS data).

Well Name	A002 ST1	A004	A007
API Number	608074062402	608074013300	608074064600
1994	5773165	--	--
1995	8304759	1040193	--
1996	4545172	1764214	--
1997	2701088	289359	--
1998	570540	2140965	321596
1999	2078339	1064467	1722169
2000	540457	191580	416778
2001	0	0	144446
2002	0	0	112607
2003	0	0	3572
2004	0	0	0
Total	24513520	6490778	2721168

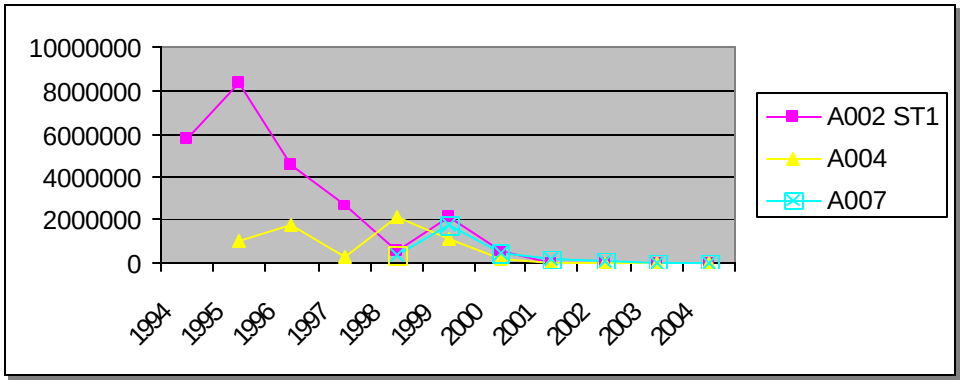

Figure 4.16: Production history in MCF for the 8500-ft sand.

4.3 Results Comparison

There is only one published interpretations for GB-191. The interpretations were published in SEG, The Leading Edge April 2000. The study was done by Chevron group (Fugitt, et. al., 2000). Although, this study plays a major role in framing my view of the GB-191, the conclusion of my thesis about sand-depositional-model and its related interpretations differ from those by Chevron group.

Fugitt, et. al. assumed that the salt mobilized before sands deposition in the Pleistocene and trapped them from going south. Also, they concluded that the 8500-ft sand is a localized channel in a small withdrawal basin just north of the salt. Therefore, the sand is restricted in GB-191. This indicates a discontinuity in the seismic reflections from sand to the south of the block.

Checking the existence of the 8500-ft sand to the south of the salt is essential to evaluate the hypothesis of Chevron group. X-lines on the extreme left side of the block show a possible continuation of the 8500-ft sand (Figure 4.17). Another evidence of continuity can be seen when viewing a seismic composite that goes from the north of GB-191 through the west part of GB-192 and finally ends at the south of GB-191 (Figure 4.18). This view simplifies the sand tracing by avoiding complex structures at the middle of the block. The previous two seismic sections doubt the idea of sand limitation to the north part of GB-191.

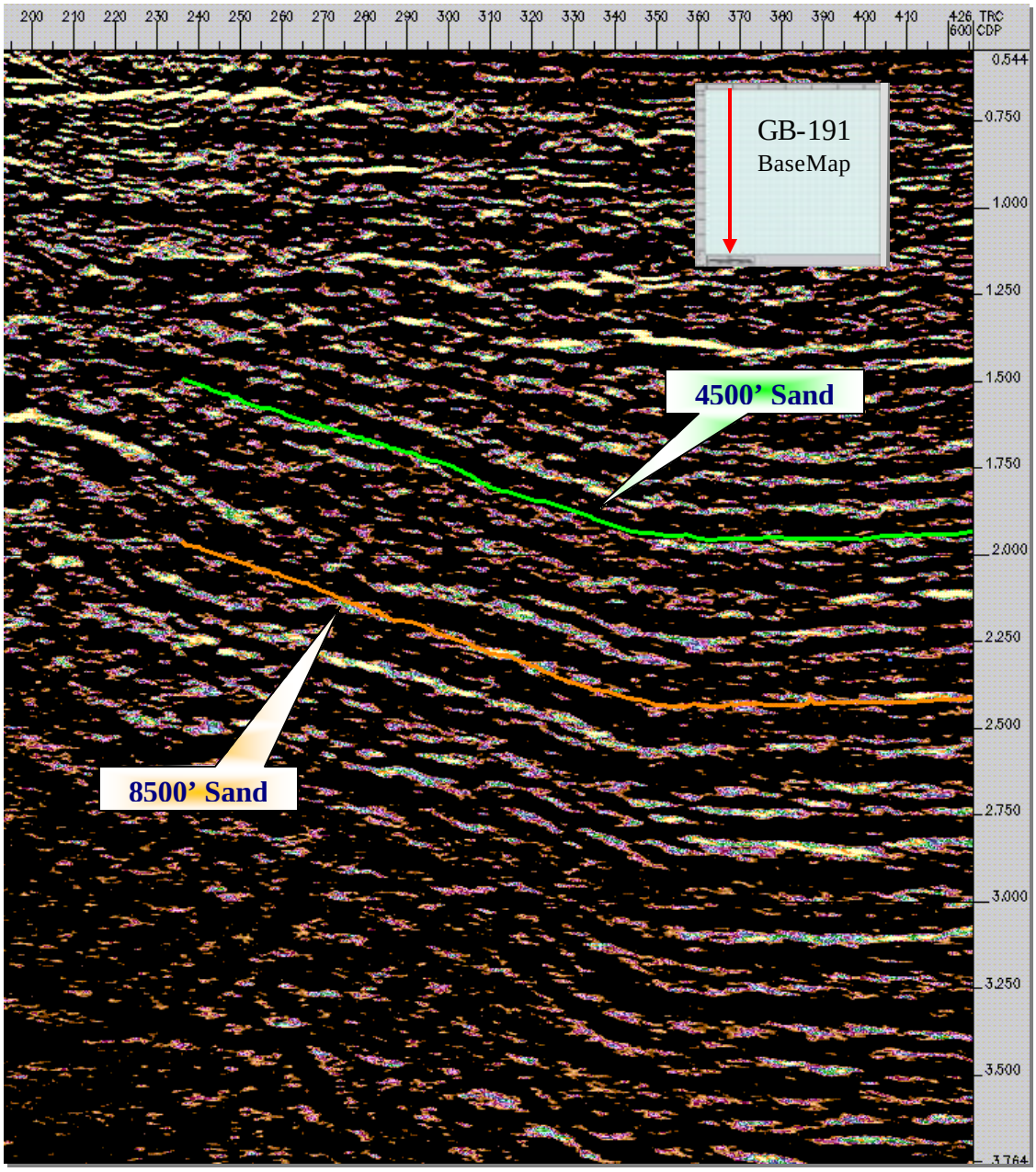

Figure 4.17: *X-line 600*
Horizontal Scale: 1:30,000 Vertical Scale: 2.5 in/sec

.

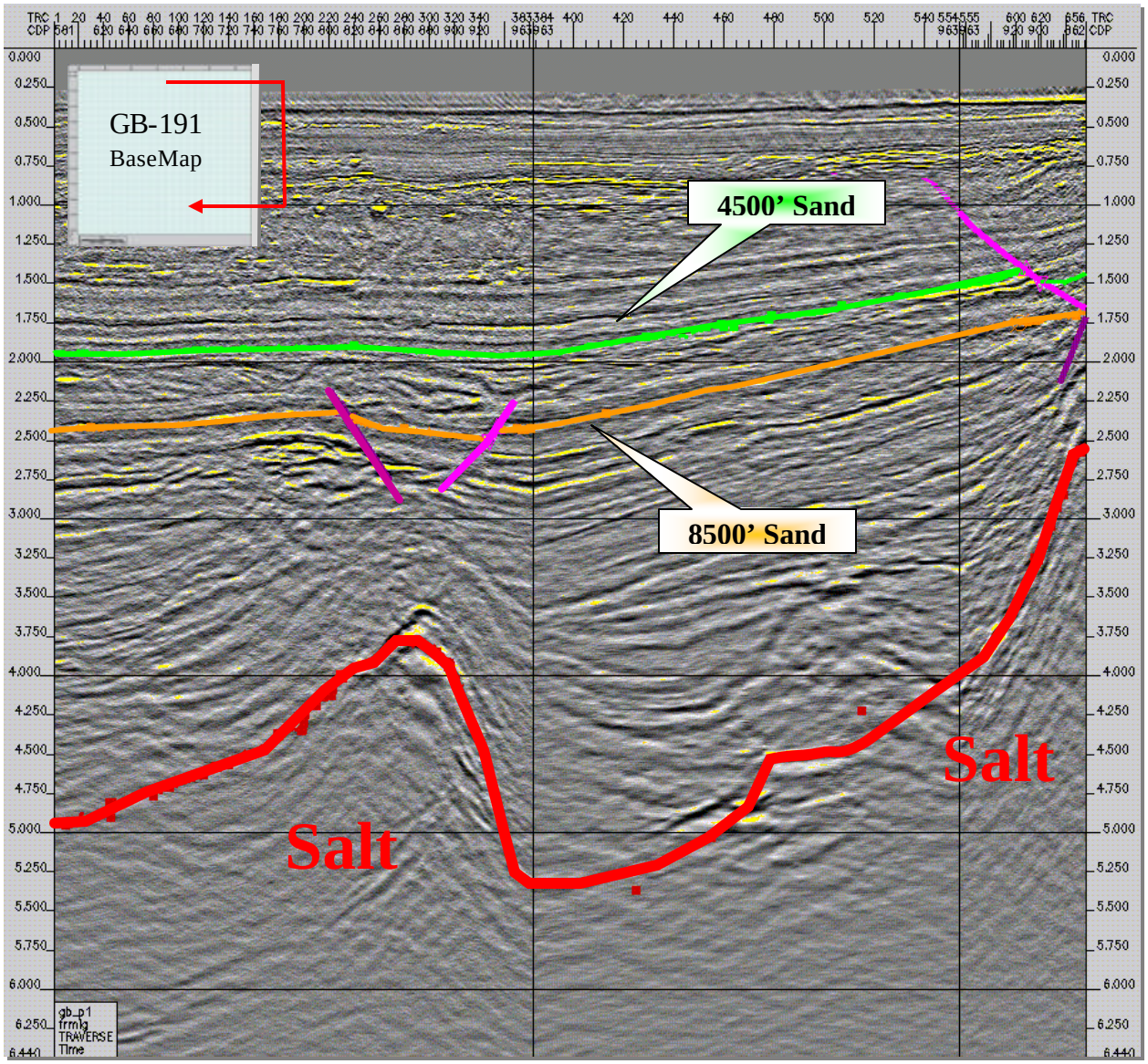

Figure 4.18: *Composite Section*
Horizontal Scale: 1:50,000 Vertical Scale: 1.25 in/sec

The asymmetric shape and the bounding fault, discussed in chapter 3, indicate that the salt is in its active piercement stage (Nelson, 1991). Usually, salt thrusts through overlaying sediments or uplifts them. In salt withdrawal areas, beds will subside and possibly be thrusted by the salt diapir. On the opposite side, beds will be uplifted. Strata, overlaying salt diapir within the uplifted area, can help in determining the thickness of layers deposited before salt evaluation. In Texas-Louisiana shelf and slope, an overburden thickness of about 5000 ft is required for salt to start rising (Nelson, 1991). According to the velocity model in the area, 5000 ft is about 1.3 seconds (average velocity of 1200 m/s). Therefore, at least 1.3 seconds of uplifted sediments should lie below the 4500-ft sand to prove that the salt diaper predated the sand deposition. This also can be justified if an unconformity in-between the 4500-ft sand and the salt peak can be found. Unfortunately, seismic doesn't prove this unconformity and X-lines show only a thin section of less than a second in-between the salt high and the 4500-ft sand. This challenges depositional model of Fugitt, et. al. A redraw of Chevron depositional model with my reading is illustrated in Figure 4.19. The model shows one scenario with the unconformity assumption. The other scenario will be similar except for the thickness of uplifted area. It will be grater than 5000 ft for both figures, 4.19b and 4.19c.

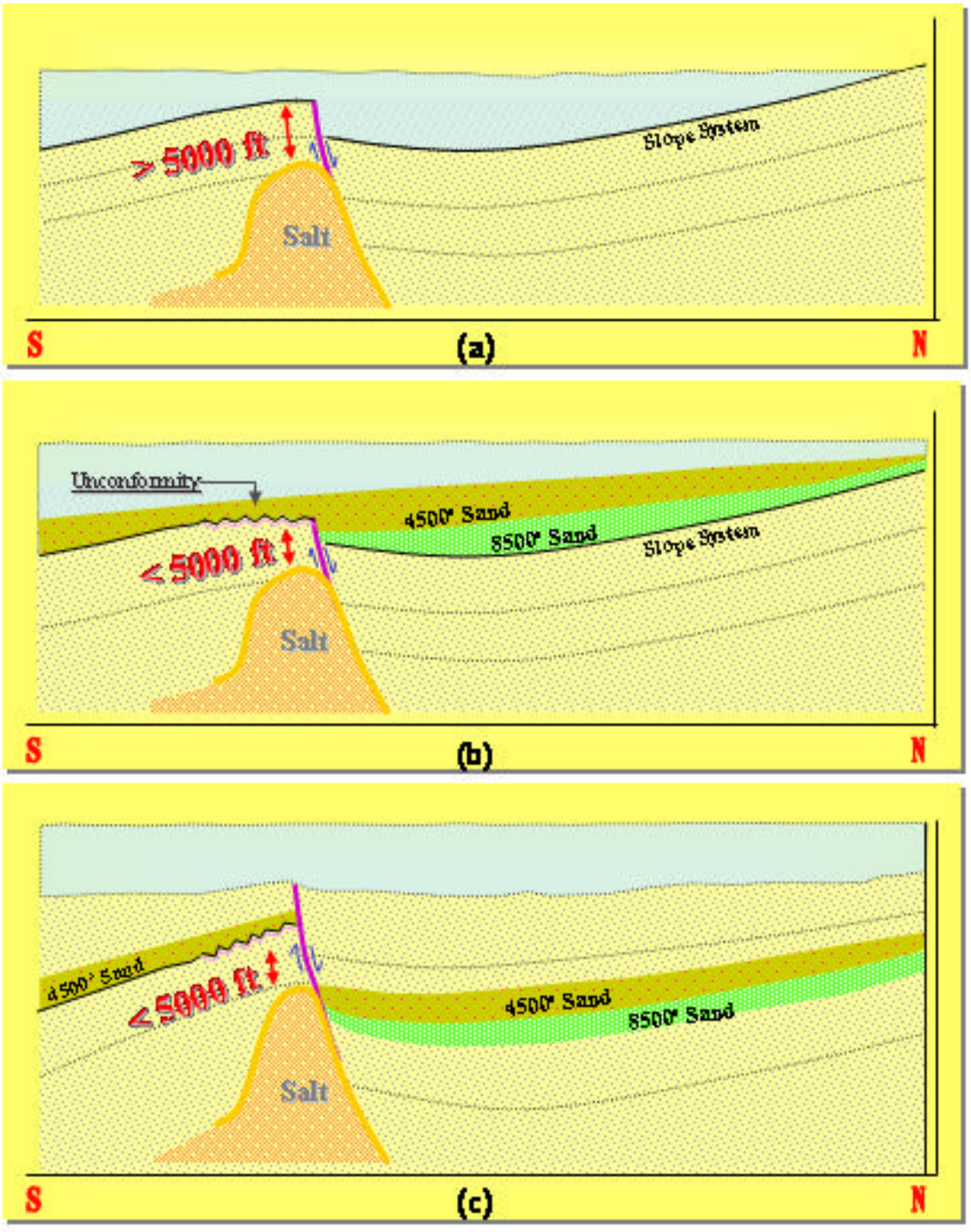

Figure 4.19: Redraw of Chevron depositional model: (a) Pre-Pleistocene view of the area. (b) Pleistocene sand deposition. (c) Post-Pleistocene extra salt mobilization.

Figure 4.20a shows Chevron interpretation for the 8500-ft sand. A normal fault cuts the block from east to west and trap the sand to the north. That fault separates between salt withdrawal area to the north and salt added area to the south. This is the main characteristic of bounding faults. I overlaid this fault over my fault interpretations in Figure 4.20b. My bounding fault runs from north-west to south-east and contradicts with Chevron fault as they are perpendicular to each other. For simplicity, I will call my bounding fault as "*fault A*" and Chevron bounding fault as "*fault B*".

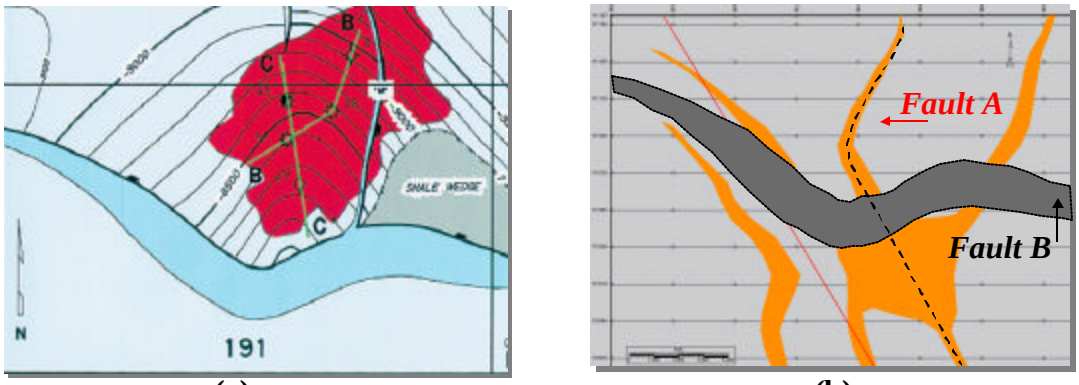

(a) **(b)**

Figure 4.20: (a) Chevron interpretation for the 8500-ft sand. (b) My fault boundary interpretation for the 8500-ft overlaid by Chevron fault.

Figure 4.21a shows a cross-sectional view for a salt structure taken perpendicular to a bounding-fault strike. The same structure will look totally different if the view is taken along the same strike (Figure 4.21b). Sections

perpendicular to the bounding-fault strike are, at the same time, along the dipping direction of uplifted strata. These sections are perfect to interpret the uplifted strata. On the other hand, sections along the bounding-fault strike present uplifted area in a shape similar to garben-horst system or anticline structure. These sections help in defining the limit of the uplifted area but can not be used in interpreting the uplifted strata.

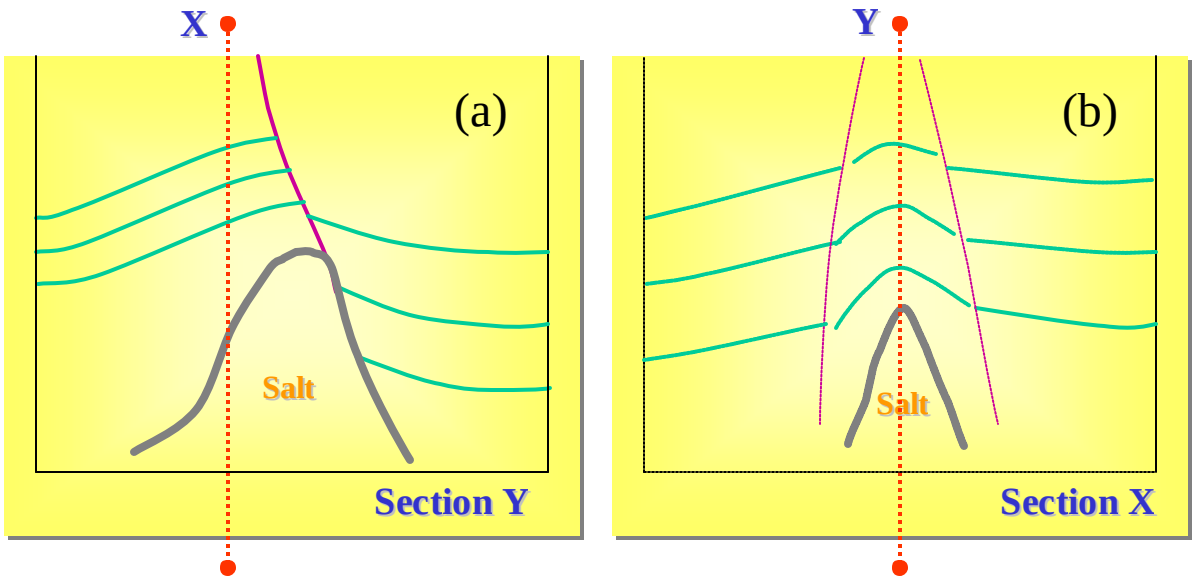

Figure 4.21: (a) Cross section perpendicular to a bounding-fault strike. (b) Cross section parallel to a bounding-fault strike.

A huge anticline shape can be seen over a traverse that is parallel to the strike of "*fault A*" (Figure 4.22). The anticline is not part of the salt limit and it is a

clear representation of the salt uplifted area. In contrast, In-lines that are perpendicular to "*fault A*" and at the same time parallel to "*fault B*", show obvious uplifted strata indicating that the cross section is parallel to their dipping direction (Figure 4.23). This eliminates "*fault B*" from being a bounding fault for the salt structure and supports "*fault A*" to be the chief fault in the area.

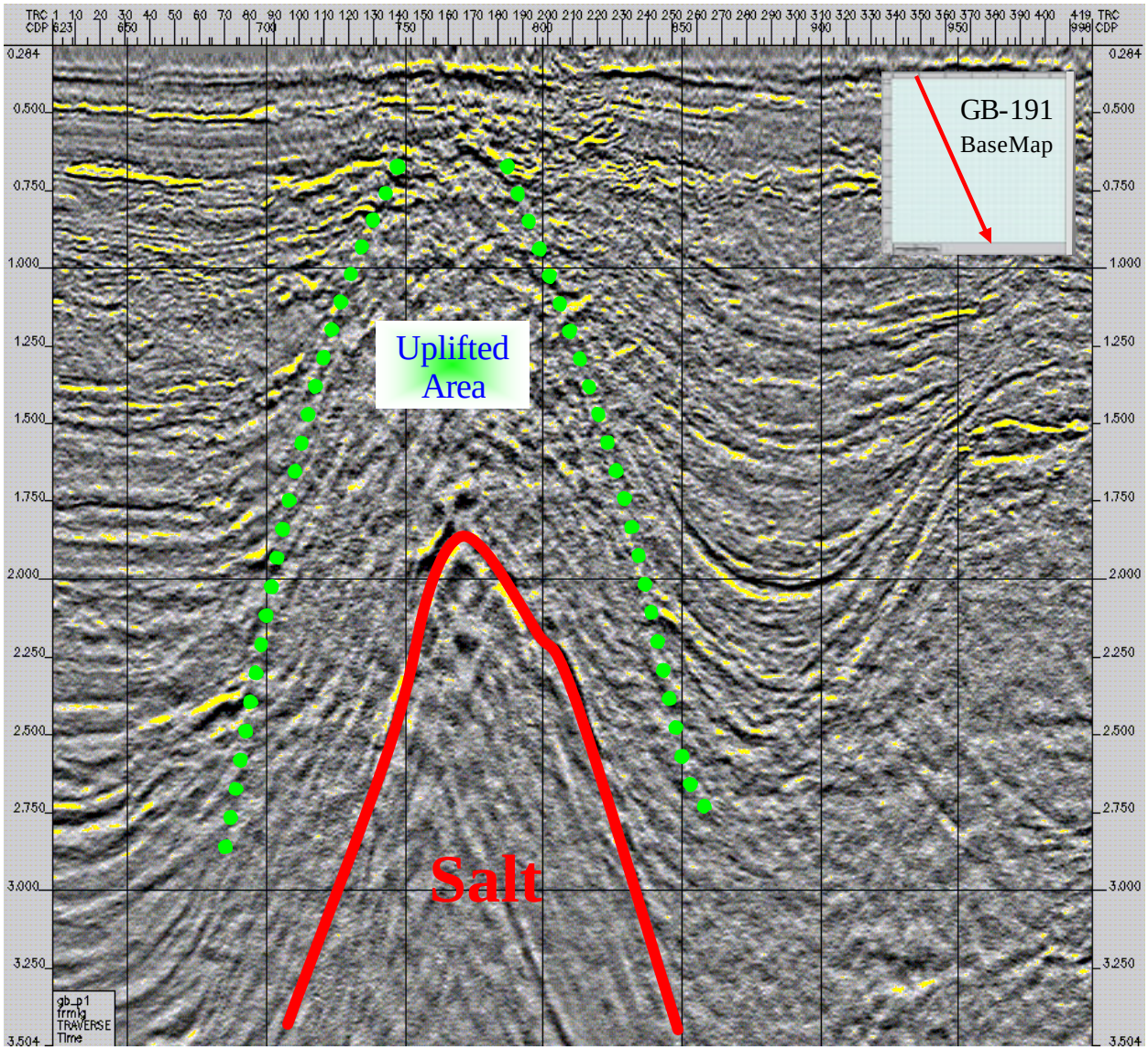

Figure 4.22: *Traverse*
Horizontal Scale: 1:75,000 Vertical Scale: 2.5 in/sec.

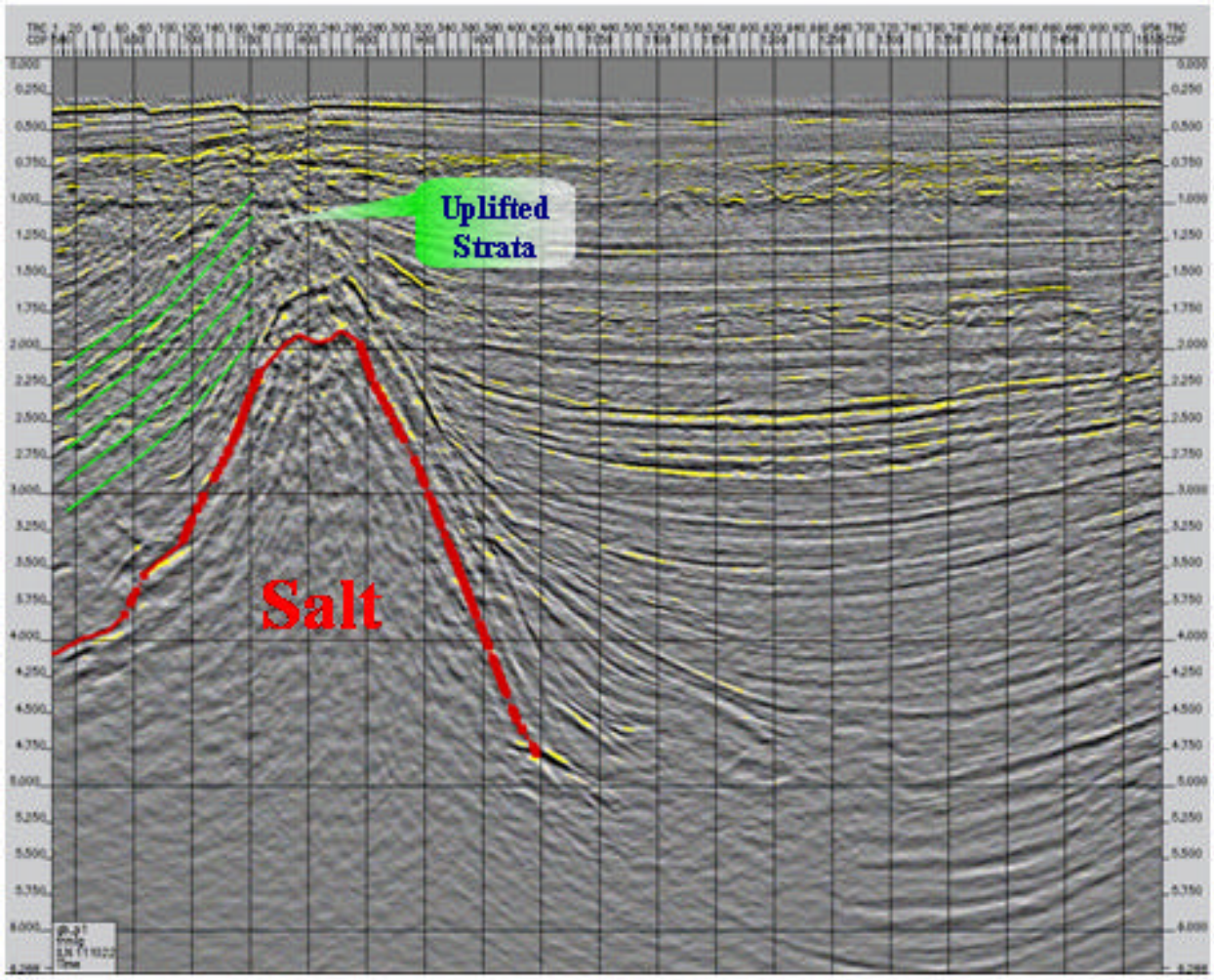

Figure 4.23: *In-line 111022*
Horizontal Scale: 1:50,000 Vertical Scale: 1.5 in/sec.

4.4 Conclusion

1) The salt diapir is still in its active stage. It splits the block into two zones, east and west. East zone strata are gently dipping while west zone strata are rotated, uplifted, and faulted.
2) A bounding fault that controls the overall structure separates the two zones. Downthrown-strata are slightly modified and pierced by the salt. Upthrown-strata, however, are uplifted and rotated but not pierced by the salt.
3) Other secondary faults are located to the left of the bounding fault in the west zone. These faults accommodated the uplift in strata within the region. As a result, they reduced the tension within the uplifted strata and introduced a new pressure over the salt-west-flank.
4) The 4500-ft and 8500-ft sands are prediapiric; deposited prior to salt evolution.
5) The 8500-ft sand is not localized in a small basin to the north of GB-191. Some evidences show a possible continuation to the south of the block.

REFERENCES

Brown, A. R., 1999, Interpretation of Three-Dimensional Seismic Data

Ewing, T. E., 1991, Structural framework, in Salvador, A., ed., The Gulf of Mexico Basin: The Geological Society of America, The Geology of North America, Vol. J.

Farmer, P., Miller, D., Pieprzak, A., Rutledge, J., and Woods, R., 1996, Exploring the Subsalt: Oilfield Review.

Fugitt, D. S., Florstedt, J. E., Herricks, G. J., Wise, C. E., Stelting, C. E., and Schweller, W. J., 2000, Production characteristics of sheet and channelized turbidite reservoirs, Garden Banks 191, Gulf of Mexico: The Leading Edge, Vol. 19, No. 4.

French, W. S., 1990, Practical seismic imaging: The Leading Edge, Vol. 9, No. 8, p. 13-20.

Link, P. K., 1987, Basic Petroleum Geology

Nehring, R., 1991, Oil and gas resources, in Selvador, A., ed., The Gulf of Mexico Basin: The Geological Society of America, The Geology of North America, Vol. J.

Nelson, A. H., 1991, Salt Tectonic and Listric-Normal Faulting, in Salvador, A., ed., The Gulf of Mexico Basin: The Geological Society of America, The Geology of North America, Vol. J.

Salvador, A., 1991, Introduction, in Salvador, A., The Gulf of Mexico Basin: The Geological Society of America, The Geology of North America, Vol. J.

Schlumberger, 1989, Log Interpretation Principles/Applications: Educational Services.

Schlumberger, GeoQuest, 2000, GeoFrame User Guide.

Tearpock, D. J., and Bischke, R. E., 2003, Applied Subsurface Geological Mapping with Structural Methods.

VITA

Omar Akbar was born on February 7, 1971. He grew up in Jeddah, Saudi Arabia. He got his B.S. degree in computer engineering from King Fahid University of Petroleum and Mineral in 1994. He joined Saudi Aramco in the same year and worked for nine years in supporting geologists with computer applications and data management. In 2005, he received a Master of Science in Geology from the University of New Orleans.